EUROPEAN COMMISSION

Community Research

RAPHAEL

Contract Number: 516508 (FI6O)

DELIVERABLE (D-CT2.6-2)

Simulation and Experimental test of AMB supported rotor with additional PMB

Author(s): **Martin GRONEK**
Frank WORLITZ

Reporting period: 15/04/2005– 14/04/2009

Date of issue of this report : 20/10/2009

Start date of project : **15/04/2005** Duration : **48 Months**

Project co-funded by the European Commission under the Euratom Research and Training Programme on Nuclear Energy within the Sixth Framework Programme (2002-2006)		
Dissemination Level		
PU	Public	
RE	Restricted to the partners of the RAPHAEL project	
CO	Confidential, only for specific distribution list defined on this document	**X**

RAPHAEL ***(ReActor for Process heat, Hydrogen And ELectricity generation)***

Distribution list

Person and organisation name and/or group	Comments
Partners of SP-CT2	
Coordinator	

ReActor for Process heat, Hydrogen And ELectricity generation (RAPHAEL)		
Sub-project: SP-CT **Work package:** 2	**RAPHAEL document no:** RAPHAEL-0906-D-CT2-6	**Document type:** D
Issued by: IPM (D) **Internal no.:** HZG-IPM-2009/610337/1.01/F		**Document status:** Final

Document title

Simulation and experimental tests of PMB supported rotor

Abstract

This document describes the results of the task Simulation and Experimental test of PMB supported rotor. The R&D work is related to the determination of the dynamic behaviour of a Hybrid Magnetic Bearing Concept (HMBC) to investigate the potentials of such bearing concept for HTR-Applications.

This report contains the subtasks of the modelling and performance of dynamic simulation calculations for the HMBC, the single effects that were indicated by the simulation calculations were also verified by the effects indicated by experimental tests of the HMBC at the FLP 500 test facility. The results of the experimental tests show that a hybrid magnetic bearing concept is feasible. The control system is able to compensate the instability and missing damping properties that are introduced by the additional PMB.

Revisions

Rev.	Date	Short description	Author	WP Leader	SP Leader	Coordinator
00	29/06/2009	First issue	Martin GRONEK, IPM	Dominique CUCINI, JSPM *Signature*	Jean Sébastien GENOT, AREVA-NP *Signature*	Edgar BOGUSCH, AREVA *Signature*
01	11/09/2009	Completing experimental investigations	Martin GRONEK, IPM	Dominique CUCINI, JSPM *Signature*	Jean Sébastien GENOT, AREVA-NP *Signature*	Edgar BOGUSCH, AREVA *Signature*
02	20/10/2009	Final Revision after review	Martin GRONEK, IPM	Dominique CUCINI, JSPM *Signature*	Jean Sébastien GENOT, AREVA-NP *Signature*	Edgar BOGUSCH, AREVA *Signature*
				23/11/09	23-11-09	23.11.09

Content

List of abbreviations

AMB	Active Magnetic Bearing
CAE	Computer Aided Engineering
HMBC	Hybrid Magnetic Bearing Concept
HTR	High Temperature Reactor
MLDia	Tool for online-diagnosis of AMB supported apllications
MLDyn	Simulation code for determining the dynamic behaviour of closed loop AMB supported rotating applications
PC	Personal Computer
PMB	Permanent Magnetic Bearing

1 Introduction

1.1 Determining the properties of a HMBC - background and goals

The development of components of High Temperature Reactors requires a major focus on safety- and reliability-related issues. That implies special requirements for the support of high speed rotating machines, which can only be satisfied by use of Active Magnetic Bearings. Due to there inherent properties AMBs are considered as key components regarding safety and competitiveness for the support of rotating HTR components.
AMBs have to be designed due to the specific requirements and operation conditions given by the machinery they should be applied to. Therefore the components of the AMB control loop has to be dimensioned and parameterized and the controller properties have to be determined by use of specific methods for non linear control loop structures.
Further components, necessary to achieve and secure the safety of the AMB supported system, are the Touch Down Bearings (also known under the term Catcher Bearing). The aim of the TDBs is to carry the shaft and withstand the loads in case of failures and emergency shutdown of the AMB support, e.g. in case of losses of energy supply. During normal operations the shaft is levitated within a small air gap and the TDBs are free of loads and rotation. When the TDBs are activated, the shaft drops down with its rotational speed. In that case the clearance between rotor and stator and the high acceleration of the TDBs mean very high mechanical and thermal loads on the TDBs. For conventional bearings the integrity and lifetime is limited by such loads. Therefore a focal point of prior investigations concerning the applicability of magnetic bearings for HTR-technology in the late 1980's was set on the reliability of Touch Down Bearings. Further references are also summarized in [1].
To meet the lifetime requirements of the TDBs it is necessary to reduce the loads acting during there activation. For vertical arranged machines a first basic approach was found by pre-centring the shaft with friction cones.
The aim of the task "Simulation and Experimental test of AMB supported rotor with additional PMB" is to investigate the dynamic behaviour and to determine the properties of a Hybrid Magnetic Bearing Concept in the context of reducing the loads on the TDBs. Hybrid Magnetic Bearing Concept means to combine Active Magnetic Bearings and Permanent Magnetic Bearings to cause synergistic effects. For those investigations a radial PMB was designed and

manufactured by FZJ [2]. For the experimental tests the PMB was mounted to the lower shaft end of the FLP 500 test bed (refer to 1.3).

This specific PMB provides an additional radial guidance of the shaft due to its radial restoring forces. In axial direction the radial PMB causes instabilities that have to be equalized by the control unit of axial AMB. The general advantages that are seen by the HMBC is the radial centring of the shaft that may reduce the loads on the TDBs and consequently the lifetime of the application may increase and the design criterions of the TDBs can be simplified.

The main goal of these investigations was to determine to what extent the HMBCs properties will be applicable for rotating HTR components.

1.2 Procedure of simulation calculations and experimental tests

To determine the dynamic behaviour of AMB supported Systems, the CAE-tool MLDyn is used. This tool allows to optimize the control algorithms and parameters due to different operational conditions of the application. Furthermore the functional requirements for the AMBs can be tested and verified by analytical experiments within those simulation calculations.

The simulation tool consist of a modular structure for each component of the AMB-control-loop. This provides the opportunity of application specific adjustments and even the implementing of additional modules like model of the PMB. The structure of MLDyn is demonstrated in Fig. 1.

To determine the necessary parameters for the simulation tool, the basic approach starts with the modelling of the magnetic bearing supported system including all geometrical and physical boundary conditions of the rotor and the AMBs. The modelling of the PMB and the determined main parameters will be presented in chapter 2 of this report.

The experimental tests have to be performed on the FLP 500 test facility (ref. 1.3). The aim of those experiments is to validate the simulation model of the PMB in the context of the whole magnetic bearing supported rotor system. This will allow transforming the determined properties and advantages of the HMBC to further HTR-application. That could be done by performance of application specific simulation calculations with MLDyn.

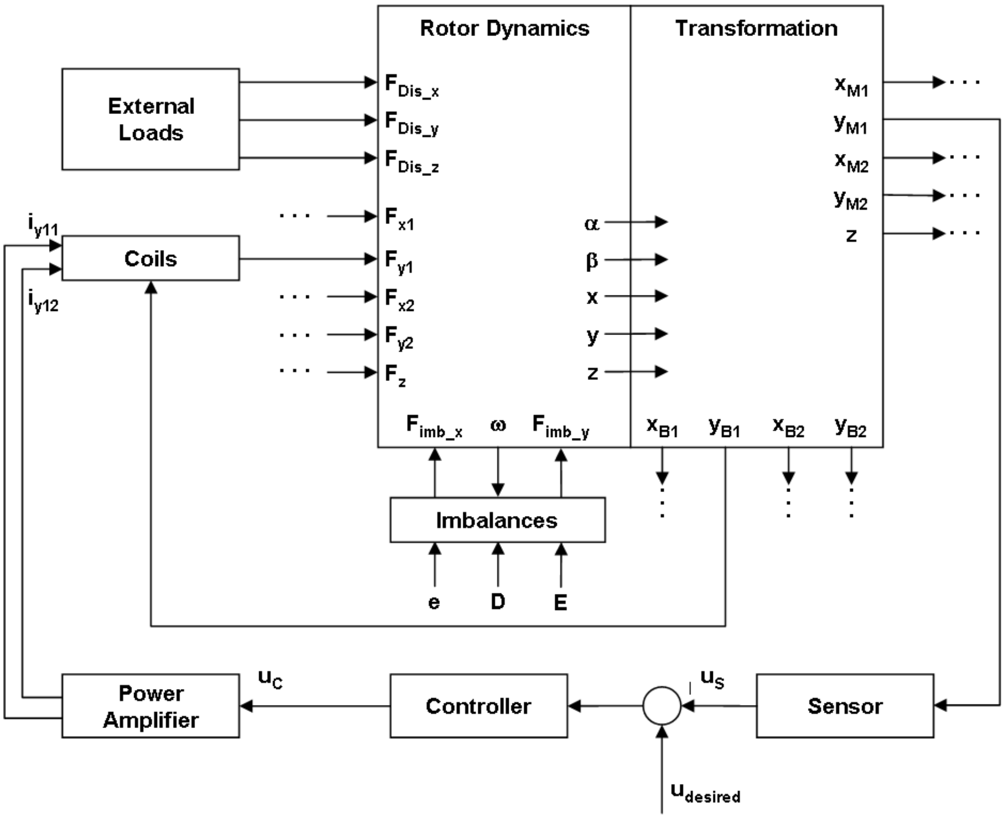

Fig. 1 : Structure of the CAE-tool MLDyn

1.3 Test facility FLP 500

The FLP 500, as shown in Fig. 2 is a vertical machine with an asynchronous motor (power: 240 kW), whose speed is controlled by a frequency converter. It was formally constructed as a test facility for TDB-investigations of a Blower application within the 80’s HTR research.
The rotor with a dead weight of 1300 kg (1500 kg with magnetic load device) is fixed completely by means of axial and radial AMBs. The maximum rotational speed is 7200 rpm. A thrust bearing as an axial magnetic bearing is located in the upper part of the machine. It consists of four ring-shaped coils and a disk at the shaft. The upper radial bearing is mounted below the axial bearing and the lower radial bearing is mounted below the asynchronous drive. For malfunctions in voltage supply, failures in control or shut down operation Touch Down Bearings are necessary to avoid damage of the rotor. There is a combined radial/axial TDB in the upper part and a radial TDB in the lower part of the machine.

Fig. 2 : The FLP 500 test facility at the laboratory of the IPM in Zittau, Germany

Each radial AMB has a redundant assembly which is moved 45 ° to the main axes and is acting in the same level. Those redundant AMBs can be used in addition to the magnetic load device for simulating mechanical loads on the shaft. A scheme of the FLP 500 is given in Fig. 3. The redundant assembly, which can be used for load simulations, is indicated at the level of the radial AMBs.

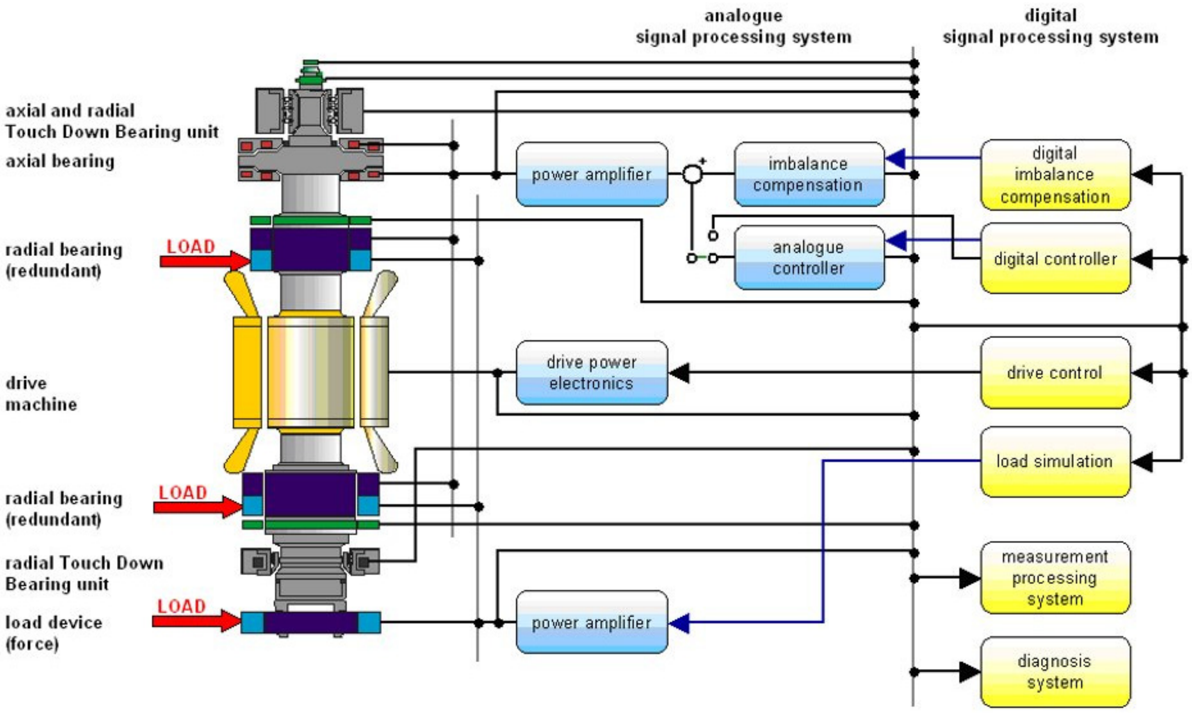

Fig. 3 : Scheme of the test facility FLP 500

For experiments with variable loads on the rotor the test facility was equipped with a special magnetic load device. It consists of three coils mounted at angles of 120 °. It is possible to simulate unit loads from external driven machines, like e.g. pumps or compressors. For the experimental investigation on the HMBC within RAPHAEL this load device was substituted by the additional PMB shown in Fig. 4.

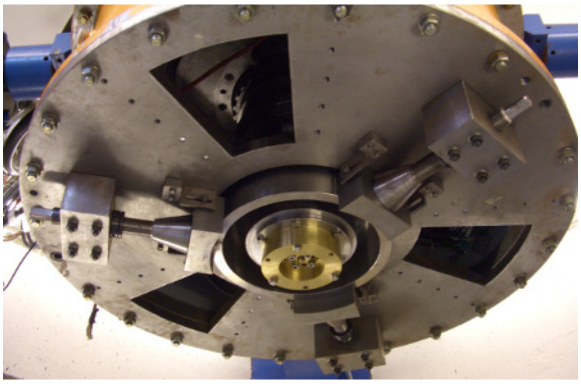

Fig. 4 : The PMB mounted on the lower shaft end of the FLP 500 test facility

2 Modelling the Permanent Magnetic Bearing

2.1 Input parameters

FZJ measured the magnetic forces between two ring-pairs in radial and axial direction. The test conditions and measurement values are given in Annex I. Based on the measurements, the characteristics were interpolated for the whole assembly.

The PMB consist of 11 stator-magnets and 10 rotor-magnets. Fig. 5 shows the sketch of the rotor-part of the PMB that was used for determining the parameter for modelling the rotor.

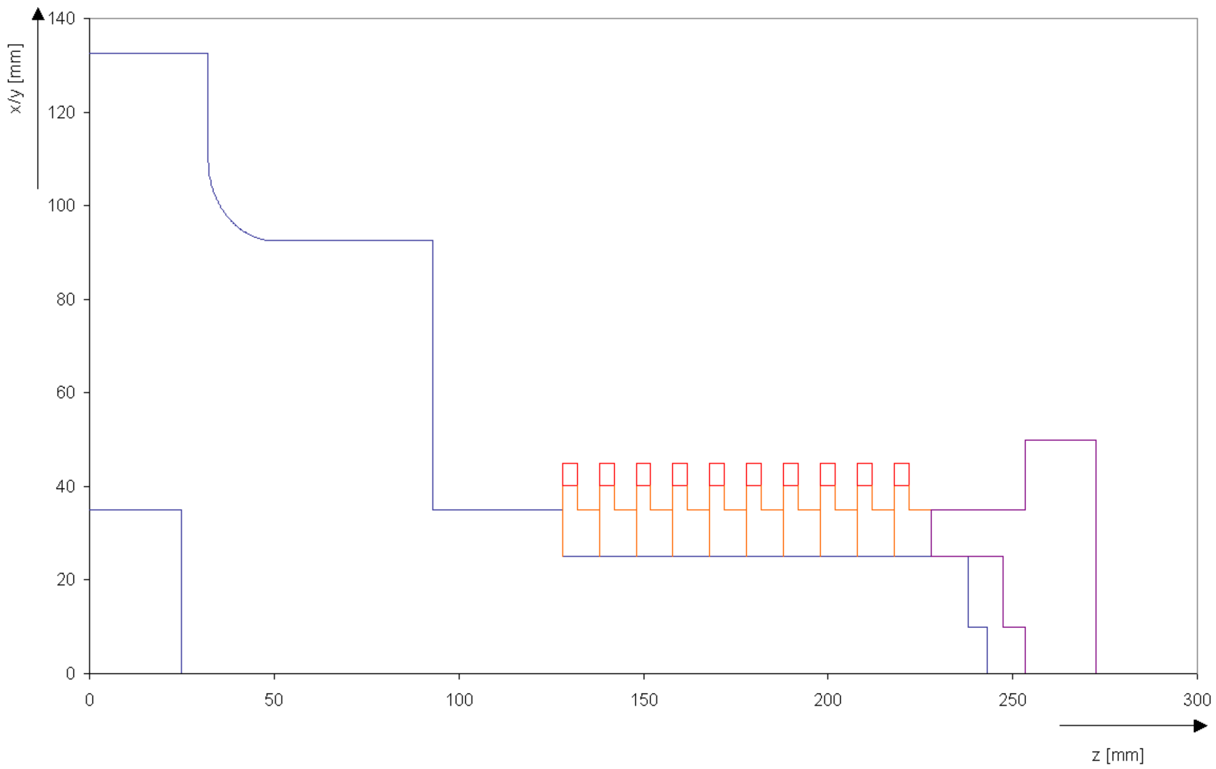

Fig. 5 : Sketch of the PMB-Rotor Part

In Fig. 5 the blue coloured line demonstrates the shape of the PMB-rotor-part ion radial direction (x/y). The orange shape characterizes the distance rings carrying the magnet rings (red). The violet shape outlines the axial stop of rotor-part – refer also to [2]. Rotor mass and moments of inertia were determined on basis of this sketch.

2.2 Static parameters

Static Parameters of the rotor model:

The static parameters were calculated from the geometric constraints and given constants for the PMB-rotor part. The necessary parameters for the model of rotor dynamics are summarised in Table 1.

Parameters	***Value***
Rotor Mass [kg]	1.336,623
Rotors axial moment of Inertia [kgm²]	23,5235
Rotors radial moment of Inertia [kgm²]	659,9889
Centre of Gravity of the complete rotor [m]	1,4729
Position of axial AMB [m]	2,4125
Position of upper radial AMB [m]	2,0185
Position of lower radial AMB [m]	0,7785
PMB position [m]	0,0945
Position of upper radial sensor level [m]	2,1735
Position of lower radial sensor level [m]	0,6235

Table 1 : static parameters of the rotor model including the PMB

Axial and radial stiffness of the PMB:

The determinations of stiffness parameters are summarized in Annex I. Due to the opposite arrangement of stator- and rotor-ring-magnets the axial and radial stiffness of the whole stack is linear.

The axial stiffness of the whole PMB assembly is:

$$\underline{\underline{-7.444,568\frac{N}{mm}}}$$

The radial stiffness of the whole PMB assembly is:

$$\underline{\underline{3.527,71\frac{N}{mm}}}$$

2.3 Implementing the PMB-Model into MLDyn

The analytical model of the PMB was implemented into the simulation tool of MLDyn. The sketch hereafter (Fig. 6) shall figure out the interfaces it has to the basic modular simulation

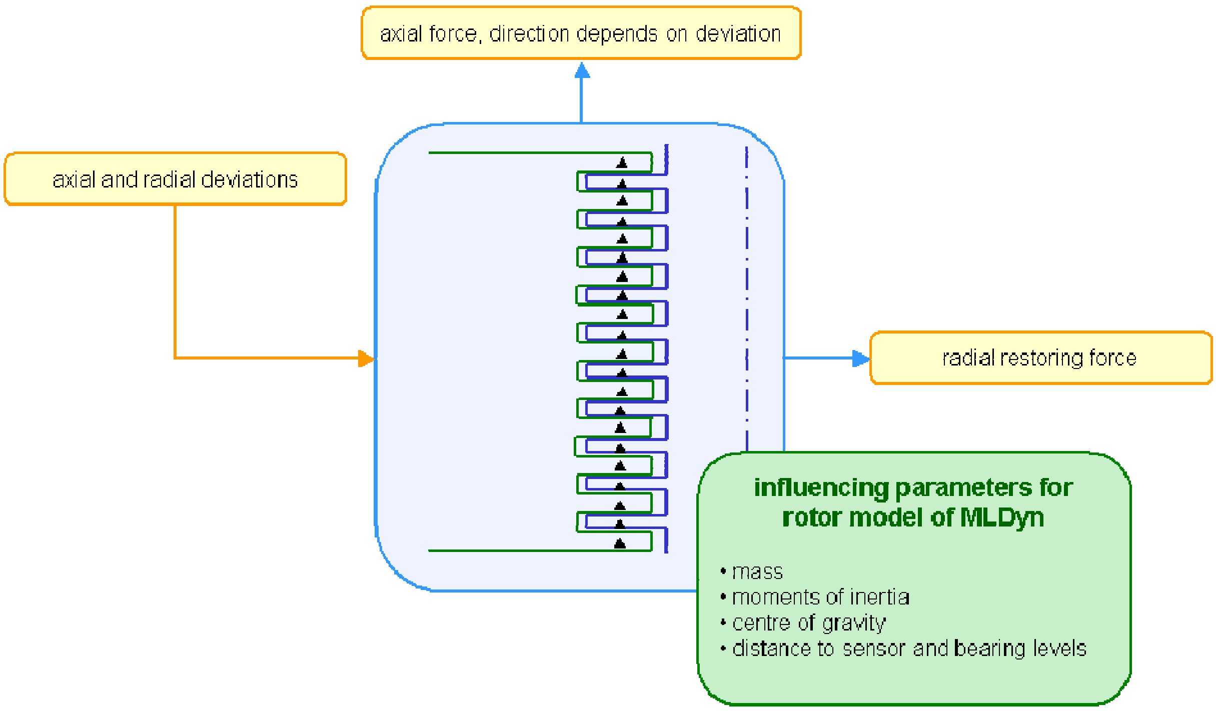

tool.

Fig. 6 : Structure and interfaces of the PMB-model

3 Performance of dynamic simulation calculations

3.1 Regular start up procedure of the FLP 500

3.1.1 How it works

The start up of the FLP 500 uses a Start-Up-Control given by a ramp-function to lift the rotor smoothly from its position in the touch down bearings up to its desired working point for levitation. The axial touch down bearing is normally stuck on the shaft due to the apply of the systems mechanical safety function. Therefore the Start-Up-Control pulls the touch down bearing down automatically by use of a lift-magnet during the start up process. This is necessary for the free rotating of the shaft due to the common operation conditions.

3.1.2 Reference simulation without PMB

To determine the influence of the additional PMB, a first calculation was performed with the model of the rotor and deactivated PMB-forces. That means, compared to the real FLP 500, to remove the permanent magnetic ring pairs of the PMB.
The following conditions were used for this simulation:

Position Parameters:

- Rotor position in the touch down bearings (axial):-0.6 mm
- Desired rotor position (final working point): 0 mm

Start-Up-Control:

The Start-Up-Control uses a ramp function to deviate the working point from the touch down bearings position up to the desired rotor position. The slope of this ramp is 0.12 mm/s to reach a rise time of five seconds from the lower to the upper limitation (-0.6 mm to 0 mm).

Controller Parameters:

During this simulation, the common PID-Controller of the FLP 500 was used with

- Controller gain: $K_r = 1$,
- Integrator time constant: $T_n = 0.25$ s and
- Deviator time constant: $T_v = 0.006$ s,

which are the original controller parameters.

Fig. 7 shows the response of the AMB-control-loop by the axial rotor position due to working point deviation.

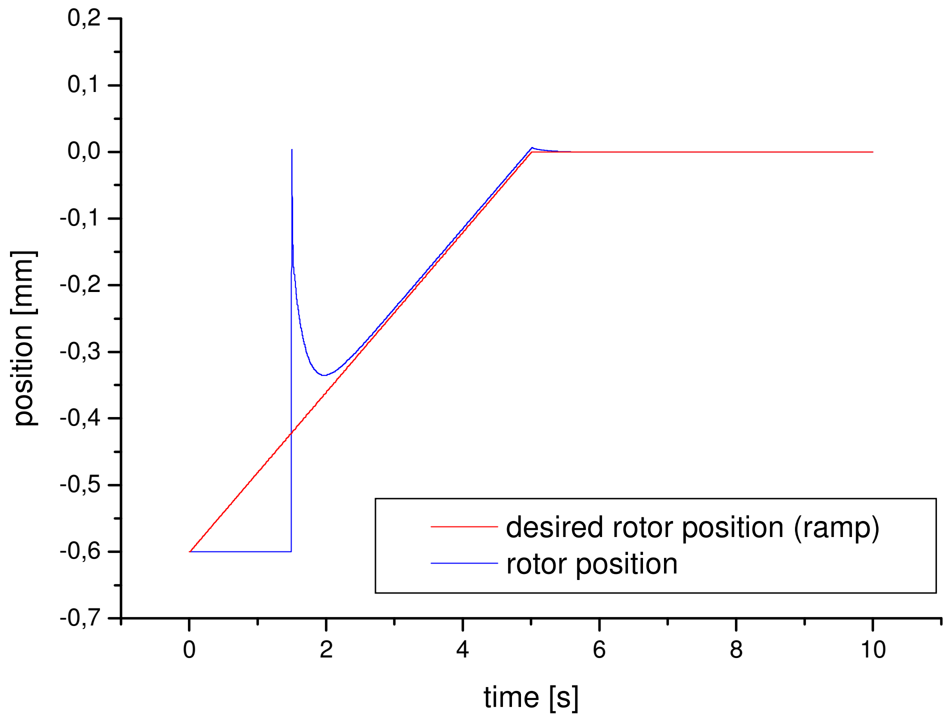

Fig. 7 : Start up process of FLP 500 without PMB at original controller parameter

3.1.3 Start up with additional PMB

First simulation calculations with the additional PMB were performed by use of the same parameters as given in subsection 3.1.2 above. In Fig. 8 is shown the ramp response of the PMB supported Rotor compared to the previous result without it. The influence of the signal noise of the position sensors was negligible for this demonstration. As can be seen on the results with the PMB, the time delay of the lifting is higher due to the attractive force that is working like additional weight when being in the position of the touch down bearing. While lifting, the rotor magnets were deviated over the critical working point, where the direction of attractive forces switches to a weight compensating force. That means, the acceleration in upward direction rises and therefore the overshoot is higher than without the PMB.

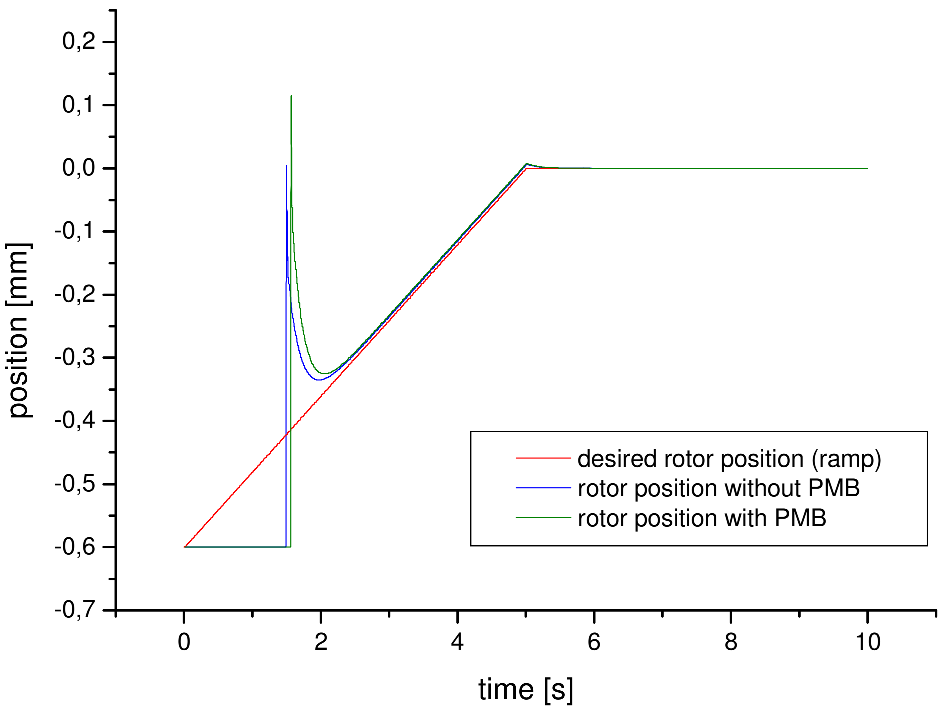

Fig. 8 : Ramp response of AMB control loop with and without additional PMB

3.2 Optimizations for start up conditions

3.2.1 General conditions

For optimization tasks it is necessary to work on the basis of constant general conditions, otherwise the results won't be comparable and at least have no meaning. Therefore the following conditions were set:

- Start up time should last 5 seconds (compare subsection 3.1.2)
- Start position at the touch down bearings (-0.6 mm)
- Final position at nominal air gap (0 mm → 0.6 mm clearance between rotor and touch down bearing)

3.2.2 Optimizing the controller parameter

To estimate the success of the parameter optimization, there are several criterions that have to be respected. In the case of the controller parameters, this will be the overshoot, the settling and build up time and the amplitude due to disturbances. Those criterions have to be minimized.

Optimization consists in tuning parameters (proportional/integral/derivative effects) to reach the smoothest transient (because overshoot is a cause of instabilities). Fig. 9 shows the result after several iterations, compared to the start up using the original controller parameters.

The optimized controller parameters are:

- Controller gain: $K_r = 2$,
- Integrator time constant: $T_n = 0.15$ s and
- Deviator time constant: $T_v = 0.015$ s,

As can be seen in Fig. 9, compared to the start up response with the original controller parameter, the settling time and overshoot were significantly reduced. The build up time is acceptable due to the increased deviation.

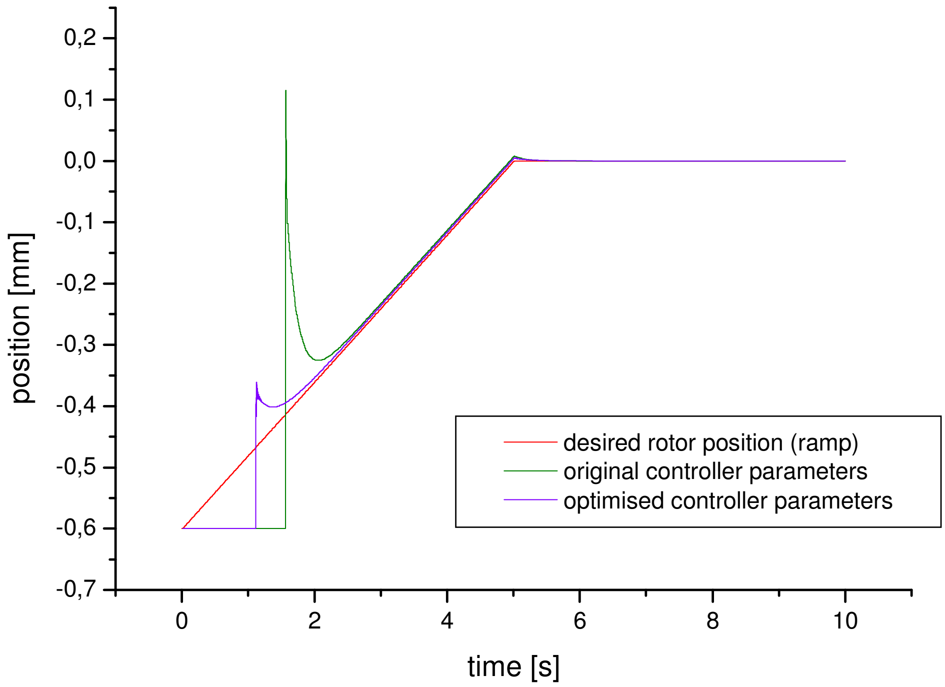

Fig. 9 : Comparison of rotor response before and after controller parameter optimization

3.2.3 Optimizing Start-Up-Control

Despite the reduced settling time and overshoot by using optimized controller parameter, the start up behaviour is not acceptable. The cause of the delay before the rotor lifts off is the slow rising of the difference between the desired and actual value of the controlled variable, while the rotor is set on the touch down bearing where the clearance to the upper actuator (lifting part) has its maximum.

This problem was solved by changing the algorithm of the Start-Up-Control. In stead of the previously used ramp, a step was combined with a ramp. The results of the previous simulation calculations showed that an optimal relation between step size and ramp is also based on the controller parameter.

The most convenient relation could be reached by a step size of half the clearance between touch down bearing and the nominal position. Smaller step sizes would result in a delay again, higher step sizes could cause oscillations up to an unstable behaviour.

Further controller optimizations were performed in addition to the optimized Start-Up-Control algorithm. The final result is given in Fig. 10. There is no delay and no overshoot in the start up response left. It reaches a settling time of 156 ms. The build up time is due to the slipped overshoot not determinable.

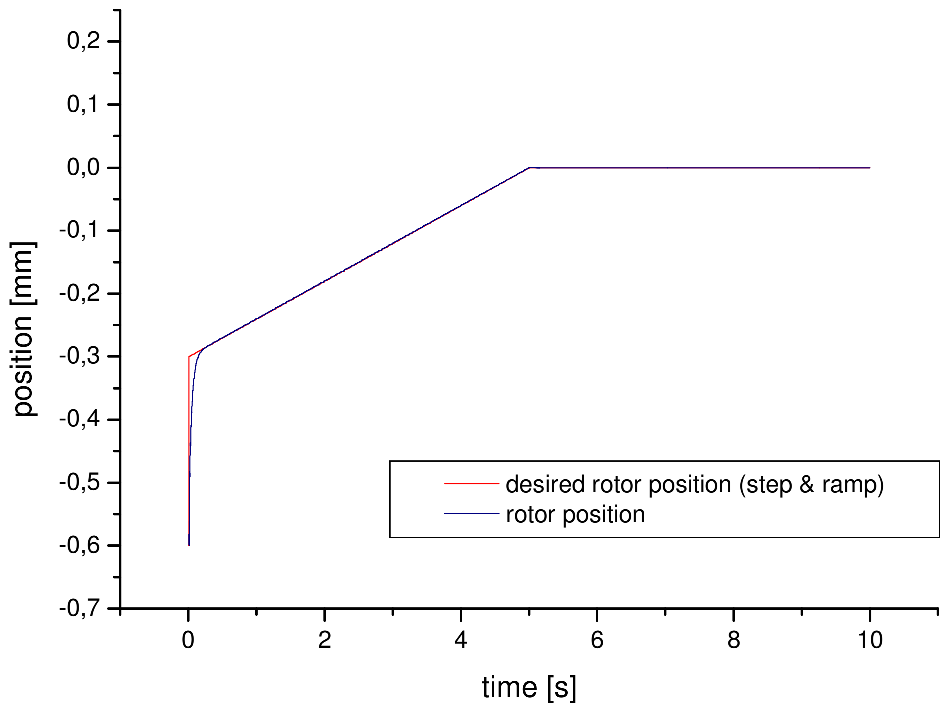

Fig. 10 : Start up response for optimized Start-Up-Control

The determined parameters are the following:

PID-Controller:

- Controller gain: $K_r = 2$,
- Integrator time constant: $T_n = 0.03$ s and
- Deviator time constant: $T_v = 0.015$ s,

Start-Up-Control:

- Step – initial value: -0.6 mm,
- Step – final value: -0.3 mm,
- Ramp – initial value: 0 mm,
- Ramp – slope: 0.06 mm/s

The output signal of the Start-Up-Control is the sum of the step and ramp signal. It is directly used as the reference value of the controlling system and is limited to a maximum value of Zero (nominal air gap).

3.2.4 Dynamic behaviour on disturbances while start up

The next step for the controller adjustment is to verify the determined parameter by use of simulation calculations in consideration of disturbances and loads, which occur during the start up process.

Inherent disturbances:

First of all, the signal noise of the position sensors is activated in the simulation model. This will demonstrate the influence of inherent dynamic disturbances. Except of the flaring noise, overlaying the position signal, it has no influence on the dynamic behaviour and the control loop, as can be seen in Fig. 11. The noise could be compensated by use of low pass filters as they will be used on the test facility later on, by now the start up response is considered as worst case estimation.

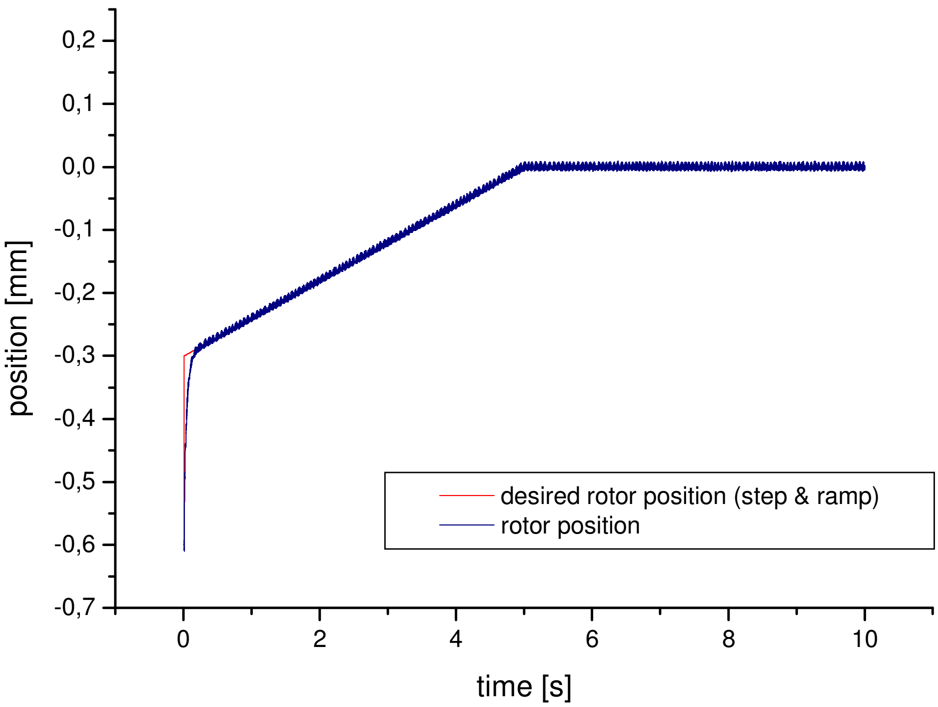

Fig. 11 : Start up response with signal noise on position sensor

Loads:

As described in subsection 3.1.1, the touch down bearing stuck on the shaft and is pulled off automatically by use of a lift-magnet while the start up process. The influence is got to be a static load, acting for a short period in direction of the gravity force. Therefore it was simulated as a single pulse-function.

Fig. 12 demonstrates the influence of a static load with the following conditions:

- Start time: t = 1 s
- Amplitude: -15 000 N
- Pulse width: 0.1 s

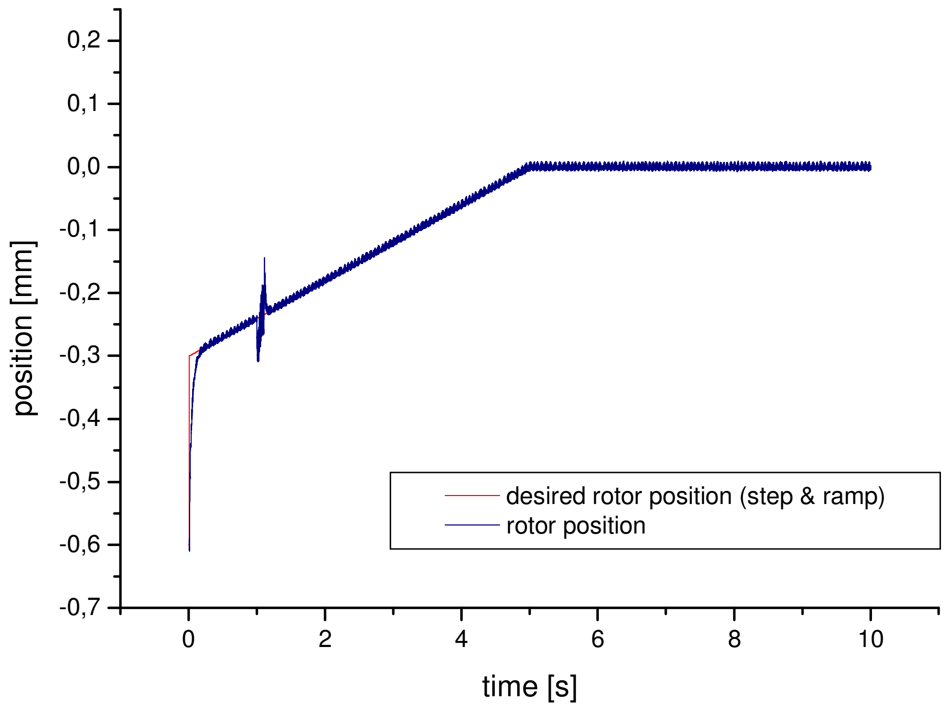

Fig. 12 : Influence of static loads

As can be seen in Fig. 12, the load causes a deviation of the rotor position in negative direction with a magnitude of 0.07 mm, the build up time is about 0.1 s. Due to the pulse width and build up time are nearly equal, a second deviation with the same magnitude in positive direction occurs, when the load is off. This deviation is also compensated by the controlling system after 0.1 s.

3.3 Conclusions on controller adjustment for start up

For the FLP 500 test facility with additional PMB, the controller parameter had to be adjusted for the start up process. Within this subtask that parameter and also the parameter of the simulation control were determined and optimized by use of simulation calculations with the specific simulation tool MLDyn.

The results of the simulation calculations are promising a stable and robust behaviour of the AMB control loop for the start up operation conditions. The success of the optimized controller parameter is demonstrated in Fig. 13 hereafter, were the optimized start up response (blue) is compared to itself by use of the original controller parameter (green).

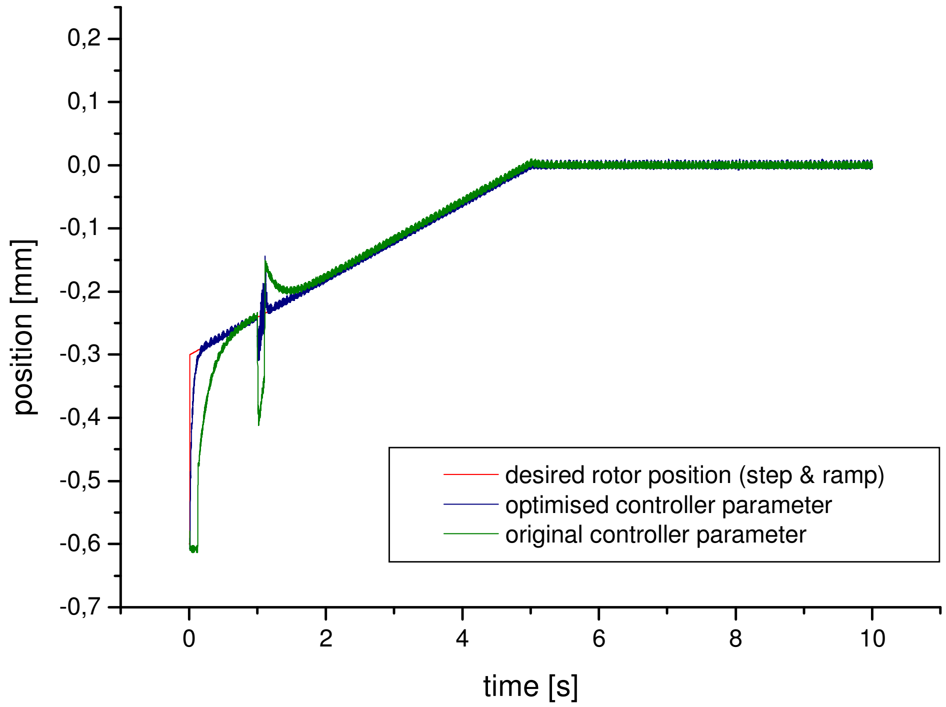

Fig. 13 : Comparison of the start up response with the original and optimized controller parameter

The next step in the working progress will be implementation of the new PID-Controller and also the adjusted Start-Up-Control algorithms on the FLP 500 test facility.

4 Experimental tests of the HMBC

4.1 Adjustments at the FLP 500 for the performance of experimental tests

After the PMB was mounted to the lower shaft end of the FLP 500 (refer to 1.3 and [2]) first start-up experiments were performed to test whether the analogue axial control unit could compensate the axial instability of the PMB. Those first tests failed [3]. This resulted in the modification of the test facility by new digital axial control system that is flexible to adjustments of controller parameters and different set-point positions of the shaft.

The necessary modification includes sensors, controller hardware, involving amplifiers and further electronic components and wiring. The axial control system works on the platform of a DSP. The control algorithms are based on a PID-Controller with additional signal filtering and anti-windup function.

For the axial AMB-control unit different parameter sets are used due to the operating state of the test facility. The operating states are divided in:

1. Start-up
2. Levitation
3. Smooth landing

The first operating state starts by the lifting of the shaft out of its arbitrary position in the TDBs to the set-point-position. If not defined to other values, the set-point-position is equal to the nominal air gap of the axial bearing, which is 600 Micrometer over the lower TDB position. When the axial shaft position reaches the set-point-tolerances, the parameter sets switch automatically.

The used parameter sets of the axial AMB-control are different for the experiment groups with and without the additional PMB. To provide a stable levitation of the shaft it was necessary to optimize the axial controller parameters for the relevant configuration of the test facility.

The control system of the lower radial AMB works for all test cases with the same controller parameter sets. This is required for comparable test results between the reference experiments without PMB and the performed tests of the HMBC. Therefore the influence of the radial restoring force of the PMB can be determined.

4.2 Scope of experimental tests and general test conditions

Goal of the experimental tests is to determine the properties of the HMBC. To differentiate the system response of the HMBC from the behaviour without PMB, the experiments have to be performed by use of the same frame conditions once with and once without the additional PMB.

The experiments are divided into the following classes:

- Start-up experiments
- Speed levels
- Static and dynamic loads
- Effect indicating tests (e.g. radial self-restoring)

The first experiment class is the start-up procedure of the AMBs. The start-up and steady state levitation is requested to different axial set-point positions for evaluating the potentials of axial dead-weight-compensation effects.

The second class of experiments tests the behaviour of the system due to inherent dynamic loads introduced by eccentricities depending on the rotational speed.

In the third class of experiments a radial load will be introduced to the shaft for different speed levels and even for n = 0 rpm.

The fourth class includes experiments to evaluate the radial restoring force of the PMB. For that it was necessary to switch off the lower radial AMB for different load cases.

The complete test and condition program is listed in Annex II.

4.3 Determination of the properties of the HMBC

The results of the experimental tests are summarized hereafter. Out of the scope of the experiments and the measured quantities the most representative data are used to demonstrate the measured effects that the additional PMB provides to the Hybrid Magnetic Bearing Concept.

4.3.1 Start-up experiments

The diagram in Fig. 14 represents the system response of the FLP 500 without PMB during the start-up procedure. In the demonstrated case the following conditions were set:

- Start-position: bottom of the TDB
- Set-point-position: nominal 0 (600 µm over start-position)
- Start-up-control function: ramp, rise time 15 sec

Fig. 15 demonstrates the same procedure with the same frame conditions but with the additional PMB on the lower shaft end of the FLP 500. The actuator current in these diagrams describes the current of the axial AMB.

Comparing those system responses, the active principle of the PMB in axial direction can be seen. The attractive force of the PMB works in direction of gravity as long as the shafts position is below the critical working point (ref. to 3.1.3). This causes at the beginning of the lift up process the longer delay until the shaft position reaches the desired position of the start-up-function.

One effect given by the additional PMB is demonstrated by the actuator current, which is directly representative of the necessary bearing force. Comparing the current effort in the state of static levitation in the level of the set-point-position it can be determined that the configuration with PMB works with a smaller current. To illustrate that, also the results of start-up experiments with set-point-position above and below the nominal air gap are demonstrated in Fig. 16 and Fig. 17 (200 µm below nominal air gap) as well as in Fig. 18 and Fig. 19 (200 µm above nominal air gap). The mean values of the current effort are summarized for these examples in Table 2.

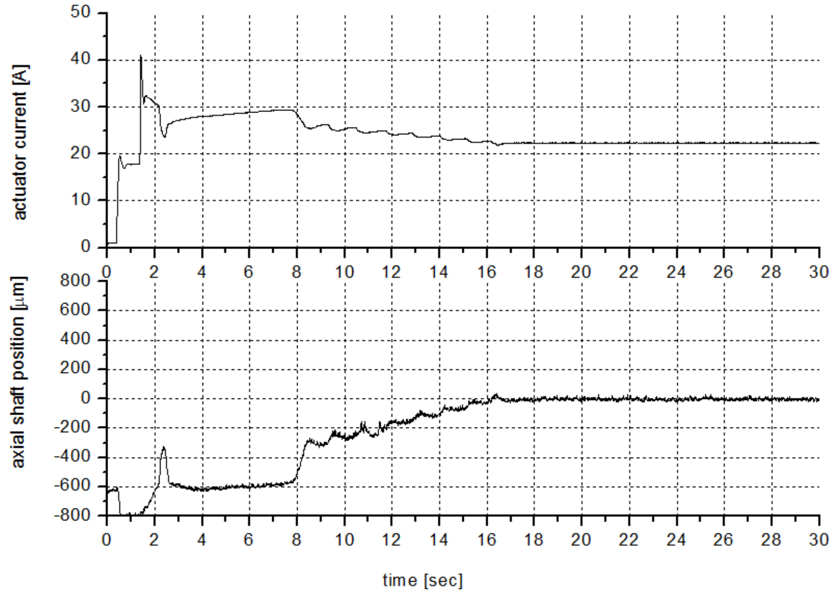

Fig. 14 : Start-up procedure without PMB, set-point-position: nominal

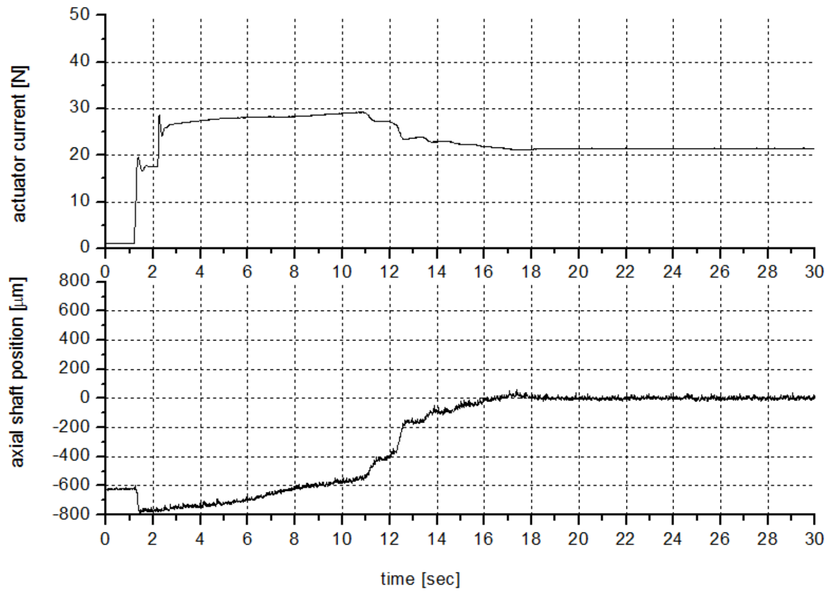

Fig. 15 : Start-up procedure with PMB, set-point-position: nominal

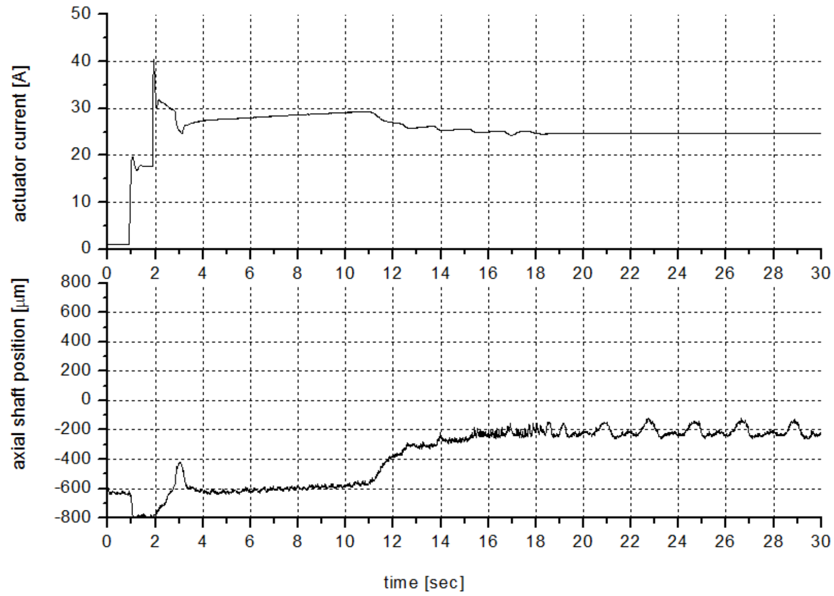

Fig. 16: Start-up procedure without PMB, set-point-position: 200 µm below nominal

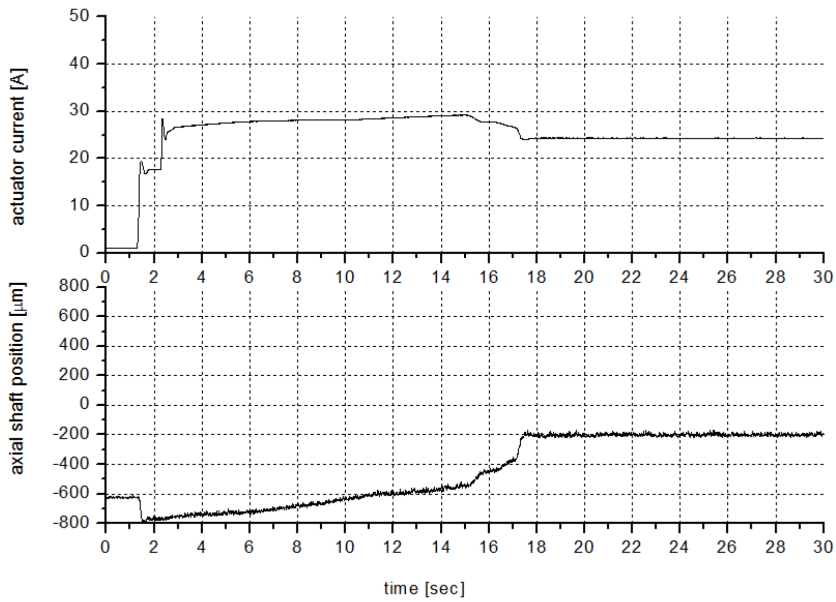

Fig. 17: Start-up procedure with PMB, set-point-position: 200 µm below nominal

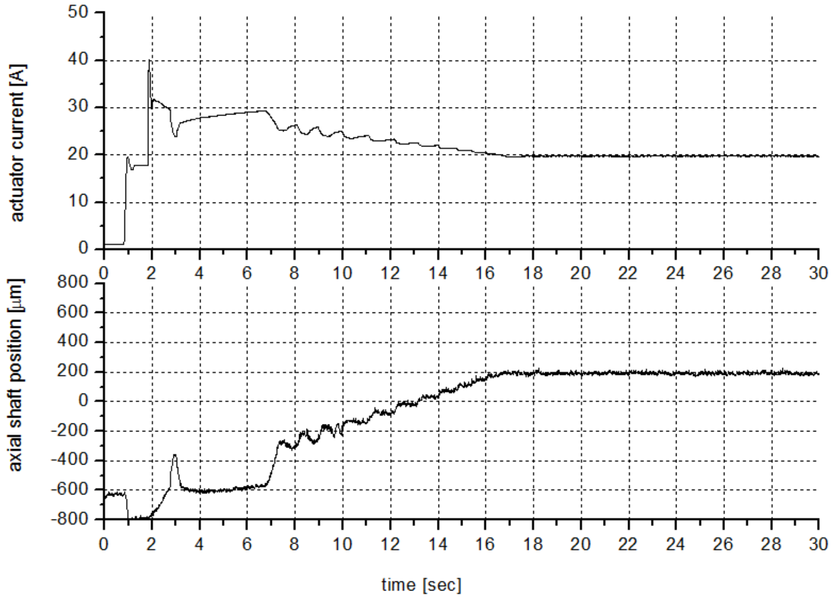

Fig. 18: Start-up procedure without PMB, set-point-position: 200 µm above nominal

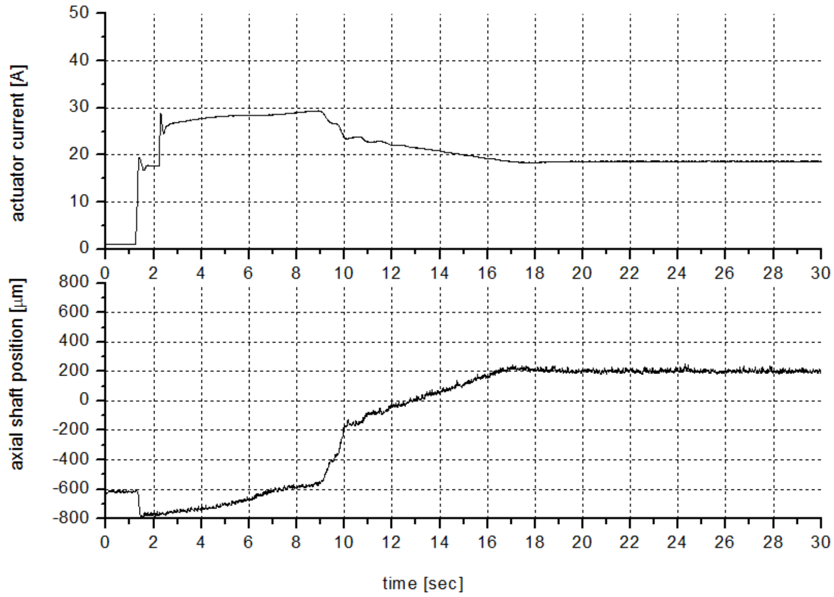

Fig. 19: Start-up procedure with PMB, set-point-position: 200 µm above nominal

Table 2: Comparison of current effort for static levitation in the set-point-level

set-point-pos.	***nominal***	***nominal +200 µm***	***nominal -200 µm***
FLP 500 configuration	***axial AMB current [A]***		
without PMB	22,35	19,73	24,68
with PMB	21,43	18,62	24,29

Table 2 shows for the first two set-point-positions that the current and therefore also the necessary force to carry the dead weight of the shaft are smaller for the case with the additional PMB compared to the other configuration. This verifies the property of the HMBC to provide dead weight compensating forces, when the set-point position is above the critical working point.

In the third example (set-point less then the nominal air gap) the set-point-position is very close to the critical working point. Critical working point meant to have the shaft position in that axial level of the PMB, where the axial forces in both directions compensate each other. This point is unstable and needs the help of the axial AMB to be stabilized by the control loop.

The critical working point was determined by interpolating from the signals of the actuator current and axial position to be app. 175 µm below the nominal air gap.

4.3.2 Speed levels

In this experiment class the influence of system inherent disturbances due to eccentricities was tested for different speed levels. The evaluation of the influence of the radial acting forces will be represented by the deviation of the shaft within the sensor level of the lower radial AMB. The first example of this experiment class has a speed of 250 rpm. In that case the amplitude with the additional PMB (Fig. 21) is smaller than without (Fig. 20). In the second case it is the other way around (Fig. 22 and Fig. 23).

For small load frequencies and amplitudes, the restoring properties of the PMB are sufficient to influence the deviation in a minimizing manner. This can be seen e.g. on the plain band in the maximum and minimum of the position signals in Fig. 21. In the second example the effect of the missing damping properties of the PMB enforces the amplitude of the deviation.

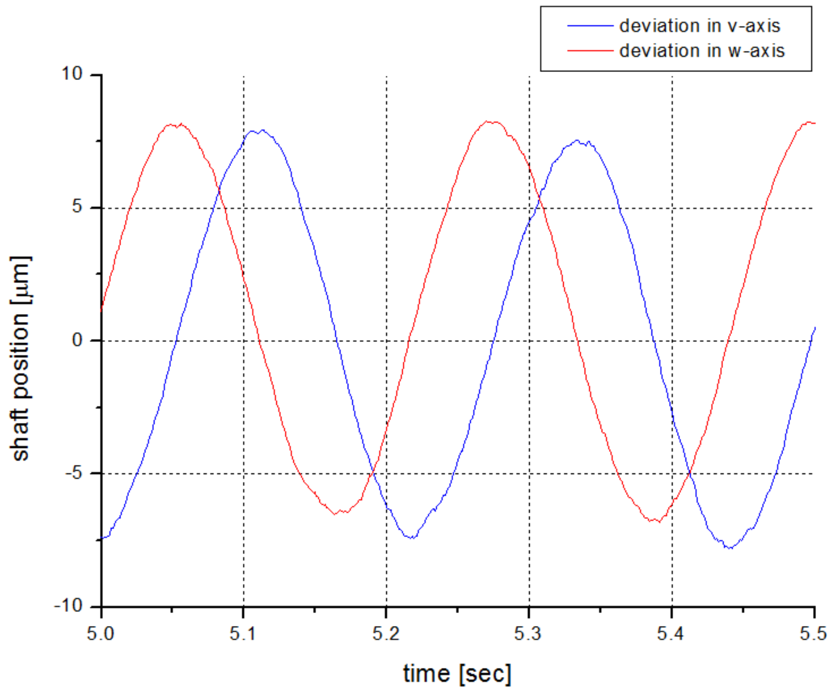

Fig. 20: Speed level at 250 rpm, without PMB

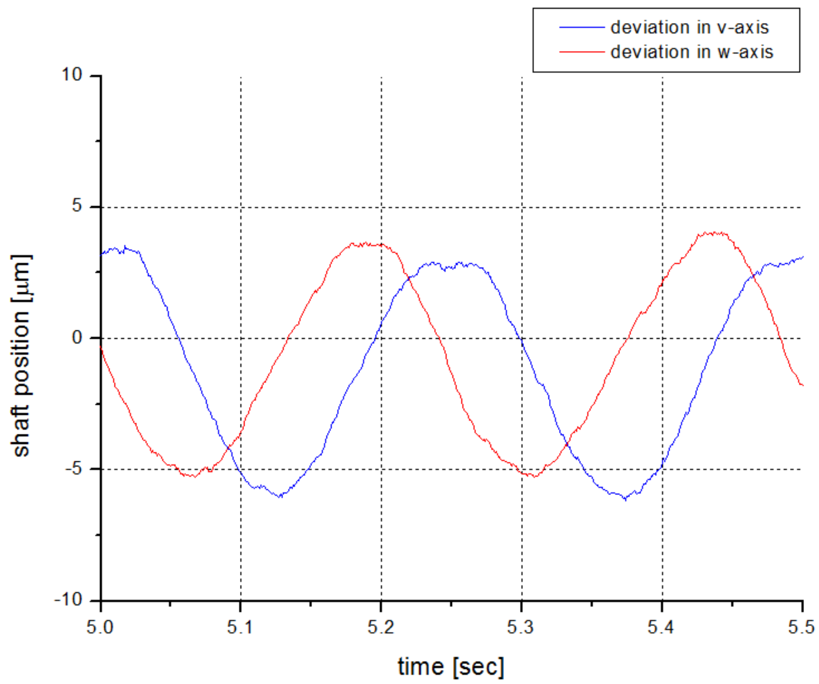

Fig. 21: Speed level at 250 rpm, with PMB

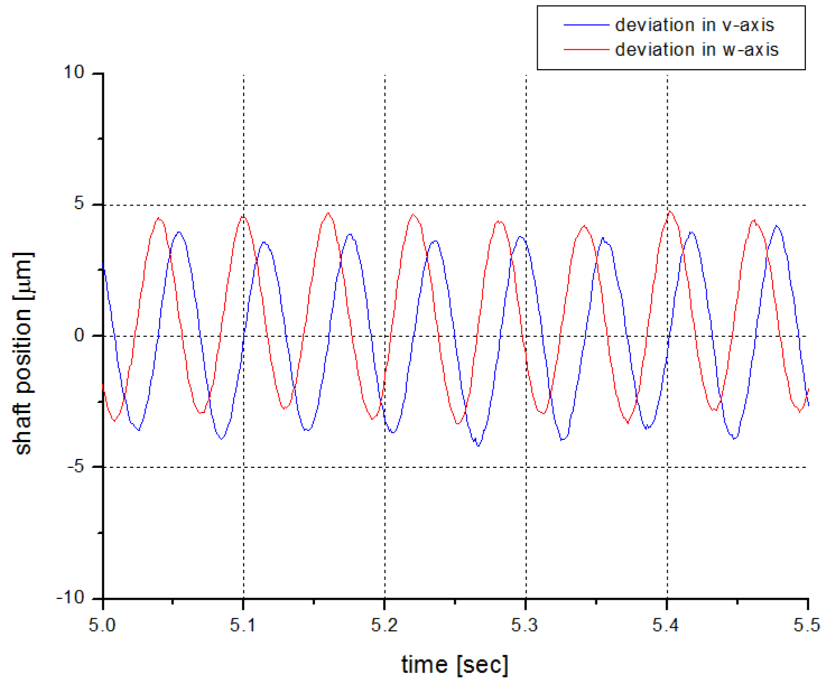

Fig. 22: Speed level at 1000 rpm, without PMB

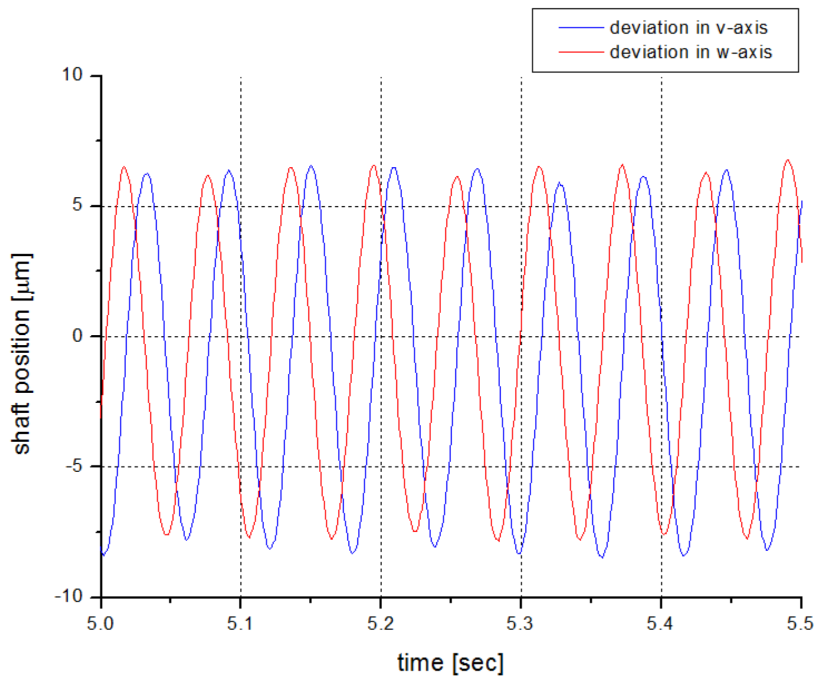

Fig. 23: Speed level at 1000 rpm, with PMB

4.3.3 Load tests

For those tests a radial load of 700 N was introduced by use of the redundant actuator assembly of the lower radial AMB. The magnitude of 700 N was chosen due to the radial stiffness of the PMB and an allowable radial deviation of 200 µm. The load of 700 N is periodically switched on and off every 10 seconds, the load direction is for both measured axes the negative direction. Fig. 24 demonstrates the static load case without PMB. Here the deviation is limited by the control system to app. -15 µm, the overshoot in the off-switched response is therefore up to 10 µm.

The same load case with additional PMB is demonstrated in Fig. 25. The PMB together with the control system limits the absolute deviation and amplitude in the off-switched response to a smaller magnitude.

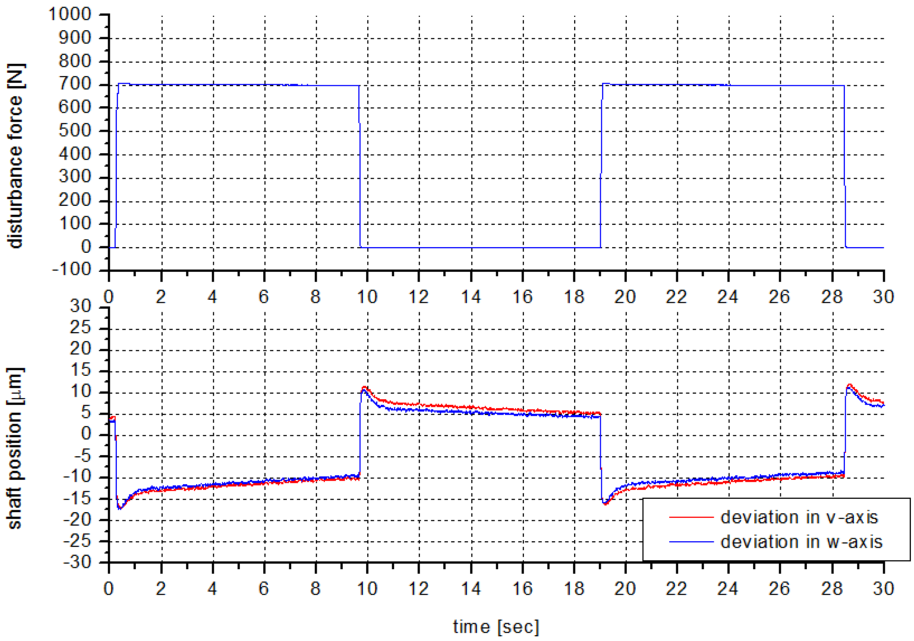

Fig. 24: Static Load 700 N; without PMB

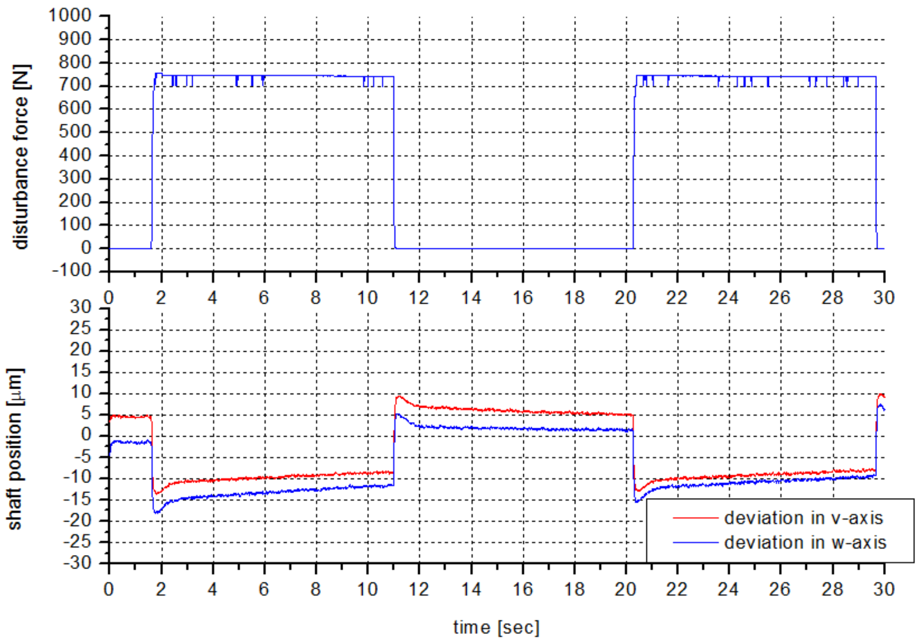

Fig. 25: Static Load 700 N; with PMB

4.3.4 Tests for indicating the radial restoring force

Due to the security barrier system those tests needed to be handled differently from normal operating modes. In a first step, a static disturbance force of 700 N was introduced on the shaft in the level of the lower radial AMB. In the second step the control system of the lower radial AMB was switched off manually (after approximately 12 seconds). For the configuration without PMB, the systems response in terms of deviation in both radial axes is shown in Fig. 26. In that case the load is sufficient to pull the shaft into the radial TDB when the radial control system fails (switched off). The repositioning that occurs after Timestamp of 13.4 sec is due to the mentioned security barrier system that automatically activates the lift magnet when the radial deviation overruns its allowable limits. This lift magnet provides a radial guidance (friction cones in contact).

The same load case, but with the additional PMB is illustrated in Fig. 27. For the load of 700 N the deviation overruns also the allowable limit and the lift magnet gets activated. But differently from the prior response, the maximum deviation does not reach the TDB and the shaft positioning is closer to the centreline of the bearing than without PMB.

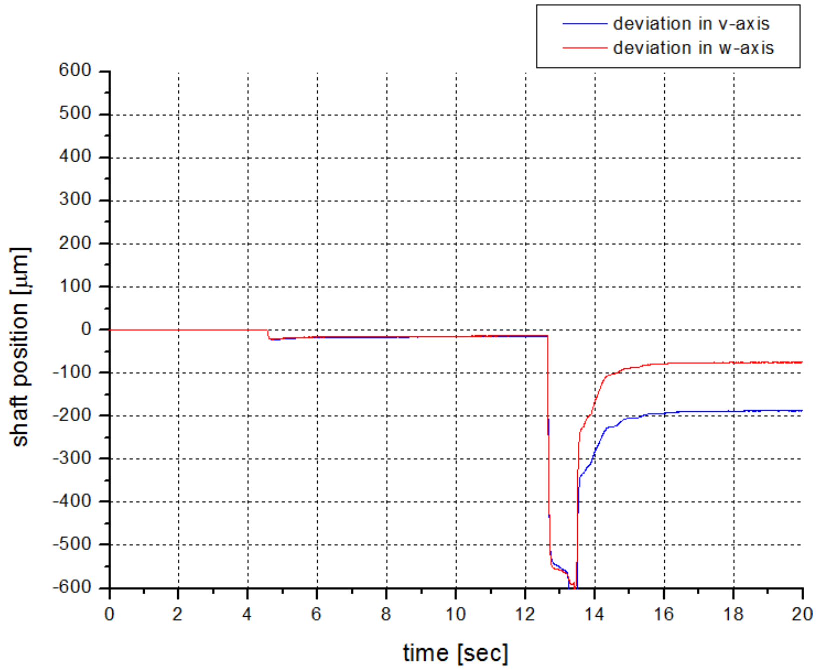

Fig. 26: Reference test without PMB: switching off the lower radial AMB at load of 700 N

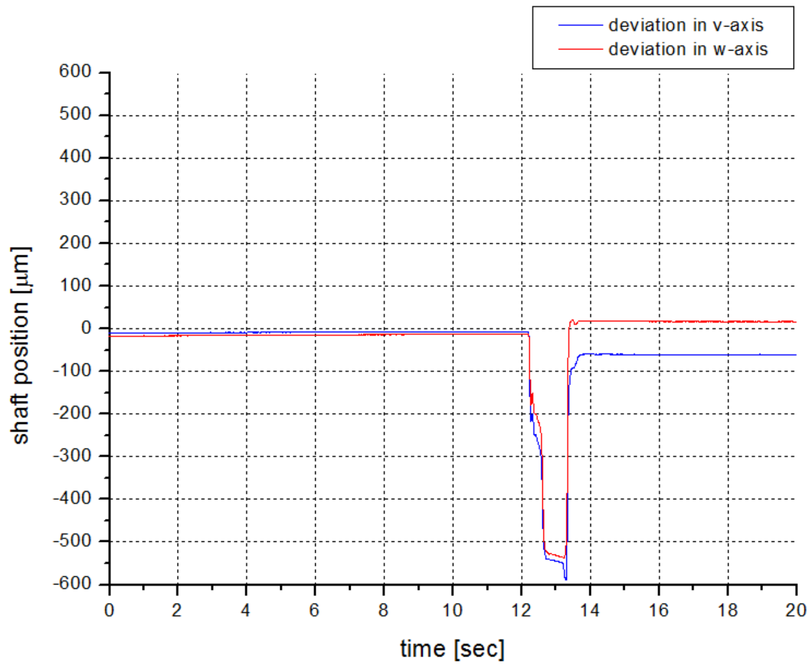

Fig. 27: switching off the lower radial AMB at load of 700 N, with PMB

The following example demonstrates the restoring force properties for the load case of 500 N (Fig. 28) In that case the PMB compensates the load regarding its radial stiffness and absolute position. Different to the previous example, the lift magnet is not activated as the deviation does not overrun its limit. Due to the PMBs restoring force the rotor is set to a new stable position.

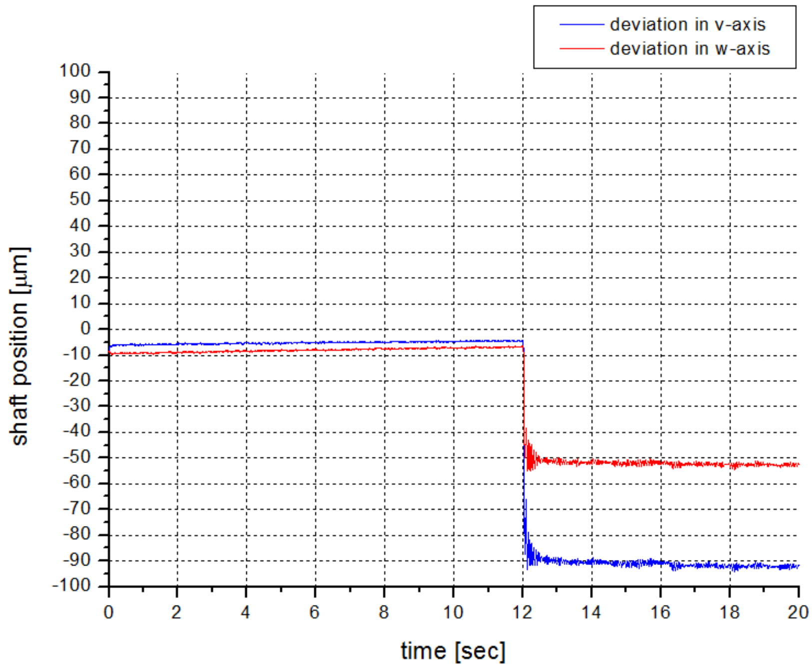

Fig. 28: switching off the lower radial AMB at load of 500 N, with PMB

4.4 Conclusions on experimental tests

The experimental tests have proven that a Hybrid Magnetic Bearing Concept is feasible and controllable. By use of the digital controller hardware (DSP) and suitable control algorithms the instabilities that are introduced by the PMB (axial direction) and also the missing damping properties of the PMB (radial direction) can be compensated. Furthermore the positive effects of the additional PMB support the vertical arranged shaft in axial and radial direction. The principles of the PMBs properties that have been outlined in the experimental tests verify the properties of the simulation models.

Defining the set-point-position of the shaft above the critical working point of the PMB, the dead weight compensating effects can be used to reduce the current effort and therefore also to reduce power losses. Further it was proven, that the axial instabilities can be compensated also in cases when the set-point-position is above or below the critical working point of the PMB.

The PMB that was used for these experimental tests was designed as a radial PMB. The reachable restoring force as a function of the radial stiffness has for the small allowable radial deviation a relative small influence compared to the load capacity of the radial AMB. Even though the experiments have shown that the PMB stabilizes the rotor within given limits when the radial AMB is switched off.

The experimental tests have proven the high potential of load reduction for the axial AMB and the TDB in case of energy losses of the Radial AMB (regarding test condition).

The results with the used radial PMB also implies the necessity to investigate the properties of radial PMBs with a higher radial Stiffness and Methods to reach damping properties of the permanent magnetic bearing (refer also to 6.1). Even in the context to safety related aspects and newly available permanent magnetic materials with higher load capacities further investigations are necessary to make definitive statements and recommendations.

5 Potentials of online-diagnosis

5.1 Diagnosis process

AMB supported rotor systems provide inherent signals that can be used for online-diagnosis methods of the applications condition and fault detection. The principles of the diagnosis process are shown in Fig. 29.

The data acquisition delivers measurement values from the technical process. In the feature extraction section, features are calculated from the variety of the single measurement values. It is assumed that changes in the process (faults) are represented by changes in the magnitudes of the features.

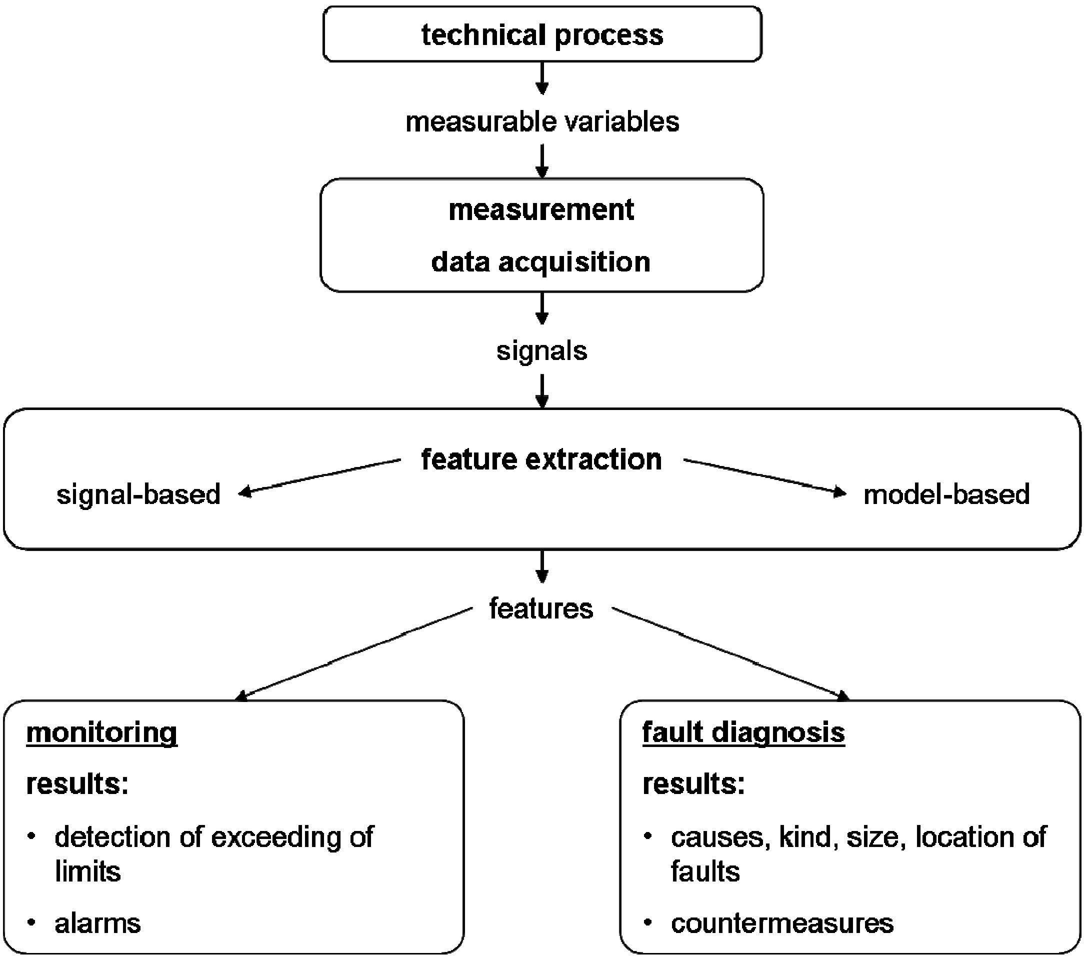

Fig. 29 : Principle of the diagnosis process

In the feature extraction there are signal-based and model-based concepts applicable. Signal-based concepts use methods of signal analysis. Model-based concepts use analytical or knowledge-based redundancy of the system to generate features which are hardly accessible by mere measurement.

The extracted actual values of the feature are monitored on exceeding of limits and trends, the exceeding of a limit characterizes the occurrence of a fault.

In the process of fault diagnosis information about the cause, size, location and consequences of the fault are generated. If possible the necessary countermeasure is to decide.

Based on this diagnosis process the realisation of the diagnosis concept is carried out in the steps:

1. Analysis of the available signals
2. Analysis and selection of feature extraction methods
3. Analysis of typical faults at components of rotating machine system with AMB
4. Acquisition of a knowledge base by simulation and experiments
5. Development, testing and verification of knowledge-based models for the fault diagnosis
6. Technical realisation on a PC

5.2 Available signals and feature extraction

At AMB supported applications the following signals are available:

- the shaft position signals s (shaft displacement),
- the actuating signals u (controller output),
- the actuating currents (coil currents),

in

- x- und y-direction of the different level radial bearings and
- z-direction (axial bearing) and
- the phase angle and magnitude of the signal vectors of each level of the radial bearings

Features can be extracted from these signals by means of signal- and model-based methods. Utilizing signal-based methods the following features are available:

- (arithmetic) mean value
- root mean square (rms)
- maximum peak value
- minimum peak value
- peak-to-peak value
- probability distribution and probability density
- auto correlation function and cross correlation function
- amplitude spectrum and characteristic frequencies

This primary features can be used to generate additional combined features:

- Ratio between the rms values of shaft displacement and the according actuating signal
- Ratio between the rms values of the actuating signal and the according coil current
- Ratio between the rms values of the opposing coil currents
- Ratio between the rms values of the positive coil current and the according shaft displacement
- Phase difference between the phase angles of the maximum signal vectors of the different level of the radial bearings

5.3 Rotating of the shaft in the touch down bearings

If the AMB is switched off and the rotor shaft rotates in the touch down bearing it is possible to detect faults and wear of the touch down bearing. Fig. 30 and Fig. 31 depict the shaft displacement orbits and the amplitude spectrum of the shaft displacement qualitatively for this case. Out of the deformation of the orbits and the characteristic frequencies information on the touch down bearing condition can be made.

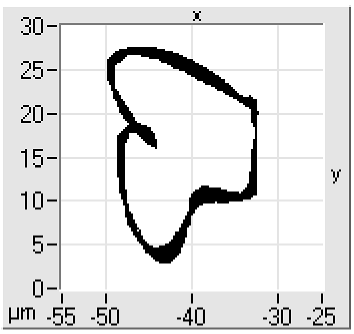

Fig. 30 :
Shaft displacement orbit
s_{yu} **vs.** s_{xu}**, AMB and motor off**

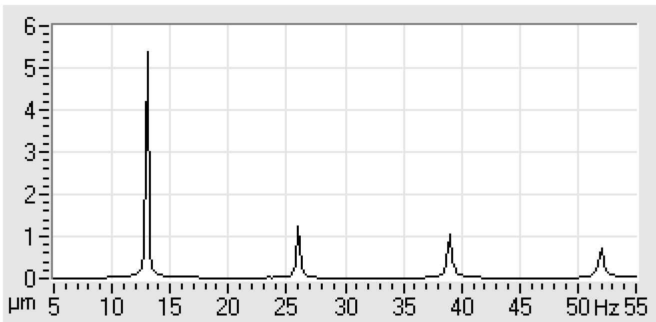

Fig. 31 :
Amplitude spectrum of the shaft displacement sxu, AMB and motor off

Significant frequencies of conventional roller bearings are:

- the bearing cage rotation frequency whose magnitude increases with cage faults
- the roll over frequency of the outer bearing ring whose magnitude increases with defects of the outer bearing ring
- roll over frequency of the inner bearing ring whose magnitude increases with defects of the inner bearing ring
- rolling elements rotation frequency whose magnitude increases with defects of the rolling elements

5.4 Monitoring

The extracted magnitudes of the features are monitored on exceeding of limits and trends. The exceeding of a limit determines the occurrence of a fault and results in an alarm. The limit value checking gives a fast way to detect critical changes of the machine condition.

Table 3 shows the used features for the limit value checking and the causes for the exceeding.

Signal	***feature***	***fault***
shaft displacement	maximum/ minimum	exceeding of the measurement range by defect of the sensor or cable circuit breaks
shaft displacement	maximum gradient	exceeding of gradients, overloading of the controller
magnitude of the shaft displacement signal vector	maximum	danger of damage by rotor-stator contact
coil current	maximum 1	Short circuit, overload of the power amplifier
coil current	minimum 1	circuit break, defect of the power amplifier
coil current	maximum 2	coil currents near the possible maximum current, nonlinear behaviour
coil current	minimum 2	coil current to low, nonlinear behaviour

Table 3 : Overview of the used features for the limit value monitoring

The main feature is the peak value of the shaft displacement. Limit value checking of the coil currents displays the occurrence of short circuits, thermal overloads and broken wires. The plausibility of the signals was checked with fixed minimum and maximum values and signal gradients. Slowly increasing faults were recognizable by calculation of the trends of the features with methods of linear regression analysis.

5.5 Diagnosis system MLDia

For the technical realisation of the diagnosis concept the diagnosis system MLDia has been developed. MLDia is modular. The present implementation comprises the modules:

- data acquisition,
- signal based feature extraction,
- parameter estimation,
- shaft displacement monitoring,
- controller output monitoring,
- coil current monitoring,
- bearing force calculation and monitoring,
- trend recording and display,
- limit value checking and adaptation,
- diagnosis.

The module **data acquisition** records a maximum of 16 channels with a sampling rate of 100 kHz which is sufficient for the diagnosis tasks. Higher sample rates and more channels are available if different acquisition hardware is used. The data acquisition records the signals shaft displacement, controller output and coil currents of the radial and axial AMB control-loops. Additionally the rotating speed is measured. In the signal **based feature extraction** the features according to section 5.2 are calculated, stored and made available for the monitoring and diagnosis. The module **parameter estimation** calculates the controller parameters of each axis. The **monitoring** modules display the main features vs. time and the orbits of the radial signals. Fig. 32 shows exemplarily a screen shot of the shaft displacement display. Limit checking barriers can be displayed in the according orbits.

Trends and gradients of selected signals and features are calculated, recorded and displayed with the module **trend recording and display**. The generating of long term trends is realised with the calculation of the mean values over a variable time. This mean values are also used for the adaptation of limit values.

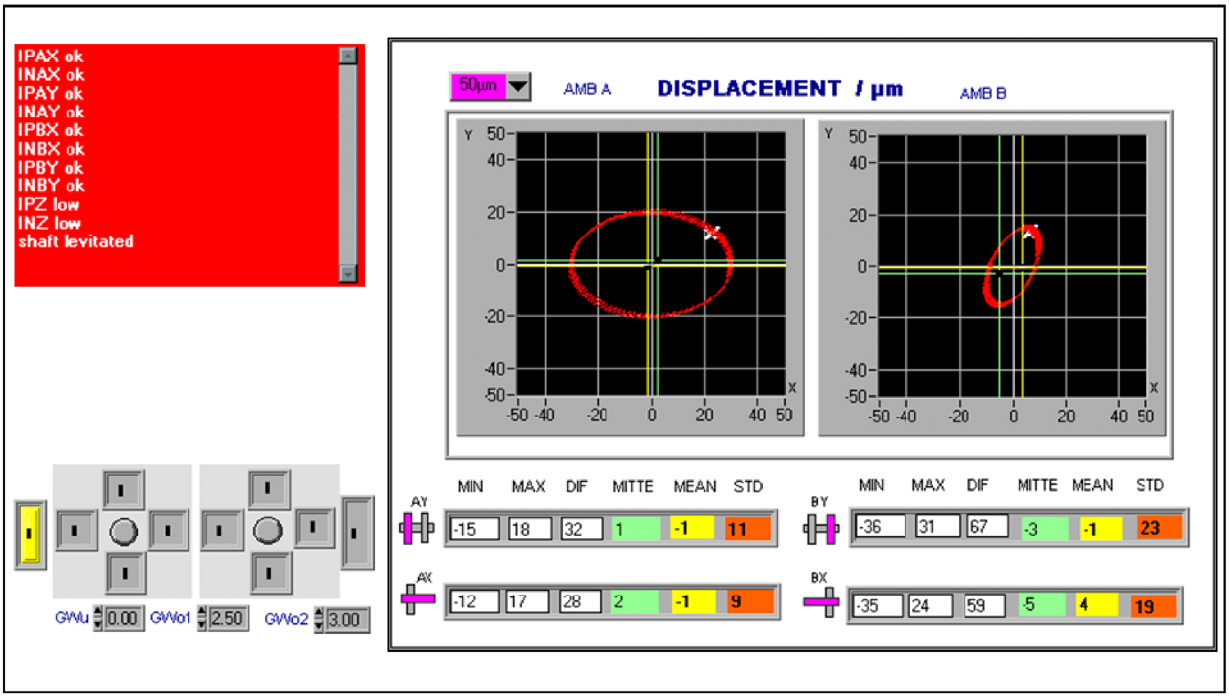

Fig. 32 : Shaft displacement monitoring in MLDia

The **limit value checking** is carried out for the mean values, rms values and the minimum and maximum values of the shaft displacement and coil current signals. It is possible to adapt the limit values automatically if the machine condition is altered. That is useful for the unattended long time monitoring of experimental AMB systems. The exceeding of limits can start a recording of the signals and features and it can trigger alarms.

The module **diagnosis** uses fuzzy based models. The processing of the algorithms is carried out in sub modules. The fuzzy sets are adaptable to different machine conditions. After the fuzzification the rules are processed hierarchically. At first the fulfilment values for the faults in every axis are calculated, from these values the diagnosis results of the different levels. In a third step it is possible to use additional feature sets for the increasing or decreasing of the fulfilment degrees. At the end all diagnosis results are displayed in the order of their fulfilment degrees in a textbox.

6 Outlook to potential subjects for further investigations

6.1 Hybrid Magnetic Bearings

Investigations in RAPHAEL were focused on a Hybrid Magnetic Bearing Concept by use of a radial Permanent Magnetic Bearing (PMB) to reach an inherent centring of the shaft. In consequence of this the loads acting on the Touch Down Bearings (TDB) when activated can be reduced.

Due to the oscillations, caused by the radial PMBs instability in axial direction, the possibility of means of a passive damping should be investigated and tested on the FLP 500 test facility

As the second part, based on the results in RAPHAEL, the HMBC with an additional axial PMB for deadweight compensation should be investigated and tested

6.2 Touch Down Bearings (TDB)

To ensure the lifetime of AMB supported blower applications, the auxiliary systems have to withstand emergency shout downs. In prior German HTR-R&D programme there were requested 14 rotor droppings within 40 years.

Today's state of the art provides new concepts of Touch Down Bearings with new construction and design and new properties. Those Concepts should be investigated and tested on test beds of the University of Applied Sciences in Zittau to validate them for use on HTR applications.

In conjunction with these proposed tests, experimental work with the goal of developing efficient models for dropping scenarios. By use of those models, the loads on the TDBs can be determined and will be the basis for optimizing the design and construction of the TDBs.

Tribology investigations are recommended to evaluate the applicability of TDB-Concepts, especially under helium conditions.

6.3 Safety, Reliability and Availability

AMBs as mechatronical systems consist of several components within the closed loop with different reliabilities.

To ensure the safety, reliability and availability of AMB supported applications it is recommended to perform an analysis and evaluation of the mechanical, electric and electronic and software components of AMB systems. The Purpose of the reliability analysis is to propose measures of construction and design to improve the availability and as the basis for decision-making, whether redundancies has to be respected.

6.4 Circulator and rotating seals

The FLP 500 test facility was preliminarily designed as a helium blower drive. The construction of this completely AMB supported test facility provides the opportunity to

- test the impeller of new gas circulator designs in helium loop (determining operation parameters, loads due to operation conditions, dynamic behaviour, …) and to
- test the rotating seals in helium loop (verifying function and efficiency, determining wear)

Possible approach is to start the tests under normal atmospheric conditions with helium as the floating medium in a closed tube-loop-system.

6.5 Rotor dynamics of magnetic suspended HTR applications

To proof the safety operation of magnetic suspended HTR applications even in case of unexpected disturbances and failures it is strictly recommended for every construction to validate the rotors dynamical behaviour due to external and internal excitations with high amplitudes. Therefore simulation calculations can be performed with MADYN2000 to determine the rotor dynamics for different stiffness- and damping-parameters of the AMBs, also including additional PMBs. An example of MADYN2000 calculations is demonstrated in Fig. 33.

The investigations will be considering different operational conditions like normal operation, dropping of the shaft into the TDBs, simulation of seismic excitation and failure caused unbalances.

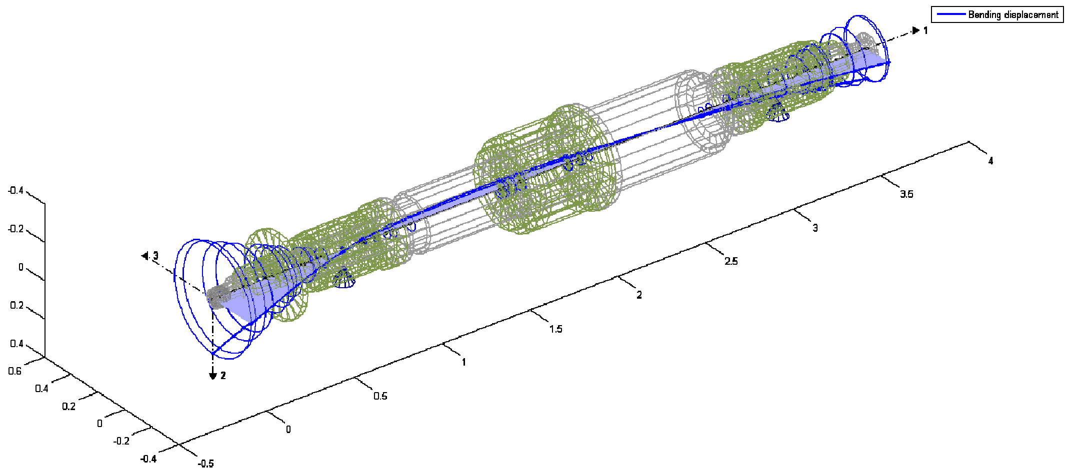

Fig. 33 : Example of MADYN2000 calculations – graphical result representation

6.6 Further potentials

The researchers of the IPM have extensive experiences in the use and development of methods, algorithms and tools of Computer Aided Engineering (CAE).

Special fields of simulation tools are used for thermodynamic and fluidic calculations including CFD (CFX).

Pooling our know how the IPM can also propose a contribution in that terms

References

[1] Lensa, W. v.: “Catcher Bearings Tests – Past experience from the German HTR R&D Programme”, Deliverable No. : 24, HTR-E-04/10-D-3-1-4-2, Juelich, Germany, 2004

[2] Lindenau, B.: “Detailed design of PMB”, Deliverable No. : D-CT2.5, RAPHAEL-06/08-D-CT2.5, Juelich, Germany, 2007

[3] Gronek, M.; Worlitz, F.: “Progress in task CT2.6”, 6^{th} RAPHAEL SP-CT progress meeting, Brussels, October, 17th 2007, Belgium, 2007

Annexes

Annex I: Determination of stiffness parameters of the PMB

Annex II: Scope of experimental tests and conditions

Annex I - Determination of stiffness parameters of the PMB

Data source provided by Forschungszentrum Juelich: Experimental tests for stiffness determination. (refer also to: *Lindenau, B.: "Detailed design of PMB", Deliverable No. : D-CT2.5, RAPHAEL-06/08-D-CT2.5, Juelich, Germany, 2007*)

Table 1: Determined forces after data-interpolation for axial stiffness

z [mm]	(2-z) [mm]	F_{ax} [N]	F(z)	F(2-z)	$F_{ax,gesamt}$ [N]
0	2	744,45676	1116,60839	-372,15163	7444,5676
0,1	1,9	670,011084	1060,78909	-390,778005	6700,11084
0,2	1,8	595,565408	1006,92731	-411,361903	5955,65408
0,3	1,7	521,119732	955,023055	-433,903323	5211,19732
0,4	1,6	446,674056	905,076321	-458,402265	4466,74056
0,5	1,5	372,22838	857,08711	-484,85873	3722,2838
0,6	1,4	297,782704	811,055421	-513,272717	2977,82704
0,7	1,3	223,337028	766,981255	-543,644227	2233,37028
0,8	1,2	148,891352	724,864611	-575,973259	1488,91352
0,9	1,1	74,445676	684,705489	-610,259813	744,45676
1	1	0	646,50389	-646,50389	0
1,1	0,9	-74,445676	610,259813	-684,705489	-744,45676
1,2	0,8	-148,891352	575,973259	-724,864611	-1488,91352
1,3	0,7	-223,337028	543,644227	-766,981255	-2233,37028
1,4	0,6	-297,782704	513,272717	-811,055421	-2977,82704
1,5	0,5	-372,22838	484,85873	-857,08711	-3722,2838
1,6	0,4	-446,674056	458,402265	-905,076321	-4466,74056
1,7	0,3	-521,119732	433,903323	-955,023055	-5211,19732
1,8	0,2	-595,565408	411,361903	-1006,92731	-5955,65408
1,9	0,1	-670,011084	390,778005	-1060,78909	-6700,11084
2	0	-744,45676	372,15163	-1116,60839	-7444,5676

Parameter z: axial distance of ring magnets

Table 2: Determined forces after data-interpolation for radial stiffness

		Restore Force $F_R(x)$ [N]										
z [mm]	**$S_{radial}(z)$ [N/mm]**	**-0,5**	**-0,4**	**-0,3**	**-0,2**	**-0,1**	**0**	**0,1**	**0,2**	**0,3**	**0,4**	**0,5**
0,000	**229,576**	-114,788	-91,831	-68,873	-45,915	-22,958	0,000	22,958	45,915	68,873	91,831	114,788
0,100	**224,257**	-112,129	-89,703	-67,277	-44,851	-22,426	0,000	22,426	44,851	67,277	89,703	112,129
0,200	**218,938**	-109,469	-87,575	-65,681	-43,788	-21,894	0,000	21,894	43,788	65,681	87,575	109,469
0,300	**213,619**	-106,810	-85,448	-64,086	-42,724	-21,362	0,000	21,362	42,724	64,086	85,448	106,810
0,400	**208,300**	-104,150	-83,320	-62,490	-41,660	-20,830	0,000	20,830	41,660	62,490	83,320	104,150
0,500	**202,981**	-101,490	-81,192	-60,894	-40,596	-20,298	0,000	20,298	40,596	60,894	81,192	101,490
0,600	**197,662**	-98,831	-79,065	-59,299	-39,532	-19,766	0,000	19,766	39,532	59,299	79,065	98,831
0,700	**192,343**	-96,171	-76,937	-57,703	-38,469	-19,234	0,000	19,234	38,469	57,703	76,937	96,171
0,800	**187,024**	-93,512	-74,809	-56,107	-37,405	-18,702	0,000	18,702	37,405	56,107	74,809	93,512
0,900	**181,705**	-90,852	-72,682	-54,511	-36,341	-18,170	0,000	18,170	36,341	54,511	72,682	90,852
1,000	**176,385**	-88,193	-70,554	-52,916	-35,277	-17,639	0,000	17,639	35,277	52,916	70,554	88,193
1,100	171,066	-85,533	-68,427	-51,320	-34,213	-17,107	0,000	17,107	34,213	51,320	68,427	85,533
1,200	165,747	-82,874	-66,299	-49,724	-33,149	-16,575	0,000	16,575	33,149	49,724	66,299	82,874
1,300	160,428	-80,214	-64,171	-48,128	-32,086	-16,043	0,000	16,043	32,086	48,128	64,171	80,214
1,400	155,109	-77,555	-62,044	-46,533	-31,022	-15,511	0,000	15,511	31,022	46,533	62,044	77,555
1,500	149,790	-74,895	-59,916	-44,937	-29,958	-14,979	0,000	14,979	29,958	44,937	59,916	74,895
1,600	144,471	-72,235	-57,788	-43,341	-28,894	-14,447	0,000	14,447	28,894	43,341	57,788	72,235
1,700	139,152	-69,576	-55,661	-41,746	-27,830	-13,915	0,000	13,915	27,830	41,746	55,661	69,576
1,800	133,833	-66,916	-53,533	-40,150	-26,767	-13,383	0,000	13,383	26,767	40,150	53,533	66,916
1,900	128,514	-64,257	-51,405	-38,554	-25,703	-12,851	0,000	12,851	25,703	38,554	51,405	64,257
2,000	123,195	-61,597	-49,278	-36,958	-24,639	-12,319	0,000	12,319	24,639	36,958	49,278	61,597

Parameter z: axial distance of ring magnets

Table 3: Determining the radial stiffness of the whole PMB assembly

			Restore Force		$F_R(x)$ [N]								
z [mm]	$k_{radial}(z)$ [N/mm]		-0,5	-0,4	-0,3	-0,2	-0,1	0	0,1	0,2	0,3	0,4	0,5
0,000	**229,576**	**123,195**	-176,385	-141,108	-105,831	-70,554	-35,277	0,000	35,277	70,554	105,831	141,108	176,385
0,100	**224,257**	**128,514**	-176,385	-141,108	-105,831	-70,554	-35,277	0,000	35,277	70,554	105,831	141,108	176,385
0,200	**218,938**	**133,833**	-176,385	-141,108	-105,831	-70,554	-35,277	0,000	35,277	70,554	105,831	141,108	176,385
0,300	**213,619**	**139,152**	-176,385	-141,108	-105,831	-70,554	-35,277	0,000	35,277	70,554	105,831	141,108	176,385
0,400	**208,300**	**144,471**	-176,385	-141,108	-105,831	-70,554	-35,277	0,000	35,277	70,554	105,831	141,108	176,385
0,500	**202,981**	**149,790**	-176,385	-141,108	-105,831	-70,554	-35,277	0,000	35,277	70,554	105,831	141,108	176,385
0,600	**197,662**	**155,109**	-176,385	-141,108	-105,831	-70,554	-35,277	0,000	35,277	70,554	105,831	141,108	176,385
0,700	**192,343**	**160,428**	-176,385	-141,108	-105,831	-70,554	-35,277	0,000	35,277	70,554	105,831	141,108	176,385
0,800	**187,024**	**165,747**	-176,385	-141,108	-105,831	-70,554	-35,277	0,000	35,277	70,554	105,831	141,108	176,385
0,900	**181,705**	**171,066**	-176,385	-141,108	-105,831	-70,554	-35,277	0,000	35,277	70,554	105,831	141,108	176,385
1,000	**176,385**	**176,385**	-176,385	-141,108	-105,831	-70,554	-35,277	0,000	35,277	70,554	105,831	141,108	176,385
1,100	171,066	**181,705**	-176,385	-141,108	-105,831	-70,554	-35,277	0,000	35,277	70,554	105,831	141,108	176,385
1,200	165,747	**187,024**	-176,385	-141,108	-105,831	-70,554	-35,277	0,000	35,277	70,554	105,831	141,108	176,385
1,300	160,428	**192,343**	-176,385	-141,108	-105,831	-70,554	-35,277	0,000	35,277	70,554	105,831	141,108	176,385
1,400	155,109	**197,662**	-176,385	-141,108	-105,831	-70,554	-35,277	0,000	35,277	70,554	105,831	141,108	176,385
1,500	149,790	**202,981**	-176,385	-141,108	-105,831	-70,554	-35,277	0,000	35,277	70,554	105,831	141,108	176,385
1,600	144,471	**208,300**	-176,385	-141,108	-105,831	-70,554	-35,277	0,000	35,277	70,554	105,831	141,108	176,385
1,700	139,152	**213,619**	-176,385	-141,108	-105,831	-70,554	-35,277	0,000	35,277	70,554	105,831	141,108	176,385
1,800	133,833	**218,938**	-176,385	-141,108	-105,831	-70,554	-35,277	0,000	35,277	70,554	105,831	141,108	176,385
1,900	128,514	**224,257**	-176,385	-141,108	-105,831	-70,554	-35,277	0,000	35,277	70,554	105,831	141,108	176,385
2,000	123,195	**229,576**	-176,385	-141,108	-105,831	-70,554	-35,277	0,000	35,277	70,554	105,831	141,108	176,385

Parameter z: axial distance of ring magnets

Annex II - Scope of experimental tests and conditions

Table 1: test program and conditions for reference experiments without PMB

No.	Axial Set-point-position	Measured quantities	speed [rpm]	load [N]	lift magnet	remarks
Experiment class 1: Start-Up experiments						
1	nominal	actuator currents, shaft position	0	0	off	
2	nominal +0,05 mm	actuator currents, shaft position	0	0	off	
3	nominal +0,1 mm	actuator currents, shaft position	0	0	off	
4	nominal +0,15 mm	actuator currents, shaft position	0	0	off	
5	nominal +0,2 mm	actuator currents, shaft position	0	0	off	
6	nominal -0,05 mm	actuator currents, shaft position	0	0	off	
7	nominal -0,1 mm	actuator currents, shaft position	0	0	off	
8	nominal -0,15 mm	actuator currents, shaft position	0	0	off	
9	nominal -0,2 mm	actuator currents, shaft position	0	0	off	
Experiment class 2: Speed levels						
10	nominal	actuator currents, shaft position	250	0	on	
11	nominal	actuator currents, shaft position	500	0	on	
12	nominal	actuator currents, shaft position	750	0	on	
13	nominal	actuator currents, shaft position	1000	0	on	
Experiment class 3: static and dynamic loads						
14	nominal	actuator currents, shaft position, control input for load	0	700	on	
15	nominal	actuator currents, shaft position, control input for load	0	1860	on	
16	nominal	actuator currents, shaft position, control input for load	0	2573	on	
17	nominal	actuator currents, shaft position, control input for load	250	700	on	
18	nominal	actuator currents, shaft position, control input for load	500	700	on	
19	nominal	actuator currents, shaft position, control input for load	750	700	on	
20	nominal	actuator currents, shaft position, control input for load	1000	700	on	

No.	Axial Set-point-position	Measured quantities	speed [rpm]	load [N]	lift magnet	remarks
21	nominal	actuator currents, shaft position, control input for load	250	1860	on	additional test
22	nominal	actuator currents, shaft position, control input for load	500	1860	on	additional test
23	nominal	actuator currents, shaft position, control input for load	750	1860	on	additional test
24	nominal	actuator currents, shaft position, control input for load	1000	1860	on	additional test
25	nominal	actuator currents, shaft position, control input for load	250	2573	on	additional test
26	nominal	actuator currents, shaft position, control input for load	500	2573	on	additional test
27	nominal	actuator currents, shaft position, control input for load	750	2573	on	additional test
28	nominal	actuator currents, shaft position, control input for load	1000	2573	on	additional test
Experiment class 4: effect indicating tests						
29	nominal	actuator currents, shaft position, control input for load	0	700	on - off	

Table 2: test program and conditions for experiments with additional PMB

No.	Axial Set-point-position	Measured quantities	speed [rpm]	load [N]	lift magnet	remarks
Experiment class 1: Start-Up experiments						
30	nominal - 0,20 mm	actuator currents, shaft position	0	0	off	
31	nominal - 0,15 mm	actuator currents, shaft position	0	0	off	
32	nominal - 0,10 mm	actuator currents, shaft position	0	0	off	
33	nominal - 0,05 mm	actuator currents, shaft position	0	0	off	
34	nominal	actuator currents, shaft position	0	0	off	
35	nominal + 0,05 mm	actuator currents, shaft position	0	0	off	
36	nominal + 0,10 mm	actuator currents, shaft position	0	0	off	
37	nominal + 0,15 mm	actuator currents, shaft position	0	0	off	
38	nominal + 0,20 mm	actuator currents, shaft position	0	0	off	
Experiment class 2: Speed levels						
39	nominal	actuator currents, shaft position	250	0	on	
40	nominal	actuator currents, shaft position	500	0	on	
41	nominal	actuator currents, shaft position	750	0	on	
42	nominal	actuator currents, shaft position	1000	0	on	
Experiment class 3: static and dynamic loads						
43	nominal	actuator currents, shaft position, control input for load	0	250	on	
44	nominal	actuator currents, shaft position, control input for load	0	500	on	
45	nominal	actuator currents, shaft position, control input for load	0	700	on	
46	nominal	actuator currents, shaft position, control input for load	250	250	on	
47	nominal	actuator currents, shaft position, control input for load	500	250	on	
48	nominal	actuator currents, shaft position, control input for load	250	500	on	
49	nominal	actuator currents, shaft position, control input for load	500	500	on	
50	nominal	actuator currents, shaft position, control input for load	250	700	on	
51	nominal	actuator currents, shaft position, control input for load	500	700	on	

No.	Axial Set-point-position	Measured quantities	speed [rpm]	load [N]	lift magnet	remarks
Experiment class 4: effect indicating tests						
52	nominal	actuator currents, shaft position, control input for load	0	0	on - off	
53	nominal	actuator currents, shaft position, control input for load	0	250	on - off	
54	nominal	actuator currents, shaft position, control input for load	0	500	on - off	
55	nominal	actuator currents, shaft position, control input for load	0	700	on - off	